Geochimica et Cosmochimica Acta, Vol. 69, No. 18, pp. 4535–4556, 2005

0016-7037/05 $30.00 + .00

doi:10.1016/j.gca.2005.03.051

A menagerie of graphite morphologies in the Acapulco meteorite with diverse carbon and nitrogen isotopic signatures: implications for the evolution history of acapulcoite meteorites

Ahmed El Goresy,[1,2,*] Ernst Zinner,[3] Paul Pellas[4,¶] and Catherine Caillet[4]

[1]Max-Planck-Institut für Chemie, J. Joachim-Becher-Weg 27, 55128 Mainz, Germany
[2]Max-Planck-Institut für Kernphysik, P.O. Box 103980, 69029 Heidelberg, Germany
[3]Laboratory for Space Sciences and the Physics Department, Washington University, One Brookings Drive, St. Louis, MO 63130, USA
[4]Muséum National d'Histoire Naturelle, Laboratoire d'étude de la matière extraterrestre, Département Histoire de la Terre, 61 rue Buffon, 75005 Paris, France

(*Received October* 26, 2004; *accepted in revised form March* 30, 2005)

Abstract—Morphologies, petrographic settings and carbon and nitrogen isotopic compositions of graphites in the Acapulco meteorite, the latter determined by secondary ionization mass spectrometry, are reported. Seven different graphite morphologies were recognized, the majority of which occur enclosed exclusively in kamacite. Individual graphite grains also rarely occur in the silicate matrix. Kamacite rims surrounding taenite cores of metal grains are separated from the Ni-rich metal cores by graphite veneers. These graphite veneers impeded or prevented Ni-Fe interdiffusion during cooling. In addition, matrix FeNi metal contains considerable amounts of phosphorous (≈ 700 ppm) and silicon (≈ 300 ppm) (Pack et al., 2005 in preparation) thus indicating that results of laboratory cooling experiments in the Fe-Ni binary system are inapplicable to Acapulco metals. Graphites of different morphologies display a range of carbon and nitrogen isotopic compositions, indicating a diversity of source regions before accretion in the Acapulco parent body. The isotopic compositions point to at least three isotopic reservoirs from which the graphites originated: (1) A reservoir with heavy carbon, represented by graphite in silicates ($\delta^{13}C = 14.3 \pm 2.4$ ‰ and $\delta^{15}N = -103.4 \pm 10.9$ ‰), (2) A reservoir with isotopically light carbon and nitrogen, characteristic for the metals. Its C- and N-isotopic compositions are probably preserved in the graphite exsolutions that are isotopically light in carbon and lightest in nitrogen ($\delta^{13}C = -17$ to -23 ‰ $\delta^{15}N = -141$ to -159 ‰). (3) A reservoir with an assumed isotopic composition ($\delta^{13}C \sim -5$ ‰; $\delta^{15}N \sim -50$ ‰). A detailed three-dimensional tomography in reflected light microscopy of the decorations of metal-troilite spherules in the cores of orthopyroxenes and olivines and metal-troilite veins was conducted to clarify their origin. Metal and troilite veins are present only near the fusion crust. Hence, these veins are not pristine to Acapulco parent body but resulted during passage of Acapulco in Earth's atmosphere. A thorough search for symplectite-type silicate-troilite liquid quench textures was conducted to determine the extent of closed-system partial silicate melting in Acapulco.

Metal-troilite spherules in orthopyroxenes and olivines are not randomly distributed but decorate ferromagnesian silicate restite cores, indicating that the metal-spherule decoration around restite silicates took place in a silicate partial melt. Graphite inclusions in these spherules have C- and N- isotopic compositions ($\delta^{13}C = -2.9 \pm 2.5$ ‰ and $\delta^{15}N = -101.2 \pm 32$ ‰) close to the average values of graphite in metals and in the silicate matrix, thus strongly suggesting that they originated from a mixture of graphite inclusions in metals and silicate matrix graphite during a closed system crystallization process subsequent to silicate-metal-sulfide partial melting. Troilite-orthopyroxene quench symplectite textures in orthopyroxene rims are clear evidence that silicate-sulfide partial melting took place in Acapulco. Due to petrographic heterogeneity on a centimeter scale, bulk REE abundances of individual samples or of individual minerals provide only limited information and the REE abundances alone are not entirely adequate to unravel the formational processes that prevailed in the acapulcoite-lodranite parent body. The present investigations demonstrate the complexity of the evolutionary stages of acapulcoites from accretion to parent body processes.

1. INTRODUCTION

Acapulcoites and Lodranites belong to an unusual group of meteorites with characteristic oxygen isotopic composition that differentiates them from other groups of primitive achondrites and ureilites (Clayton et al., 1984; Clayton et al. 1992; Franchi et al., 1992; McCoy et al., 1997a). Whole-rock oxygen isotopic compositions of acapulcoites and lodranites show complete overlap, clustering around $\delta^{18}O \sim 3.5$‰ and $\delta^{17}O \sim 0.75$‰, suggesting an origin from a common parent body that is clearly different from those of other primitive achondrites (Clayton et al., 1984; Clayton et al. 1992; McCoy et al., 1997a). There is abundant evidence that acapulcoites have chemical affinities to H-chondrites (Schulz et al., 1982; Palme et al., 1981; Zipfel et al., 1995). However, the abundances of moderately volatile elements (Au, As, Ga, Ge, Zn, etc.) in acapulcoites are significantly higher than in H-chondrites (Palme et al., 1981; Zipfel et al., 1995). Chemical compositions of silicates in both acapulcoites and lodranites lie between those in enstatite and H-chondrites (Palme et al., 1981; Zipfel et al., 1995). However,

* Author to whom correspondence should be addressed (ahmed.elgoresy@uni-bayreuth.de).
¶ Deceased.

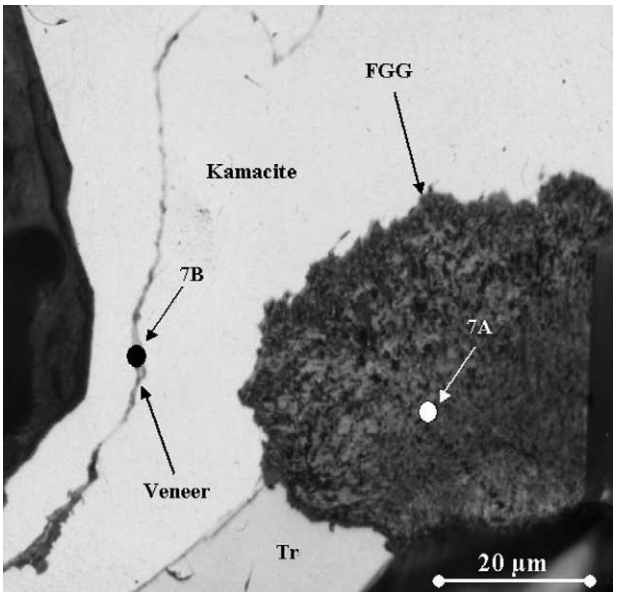

Fig. 1. A reflected light photomicrograph of an oval-shaped inclusion of fine-grained polycrystalline(different shades of gray to black are due to bireflection) graphite (FGG) in kamacite. Notice the coarsening of the graphite crystallites towards the contact with kamacite. The picture also shows a veneer of graphite books between kamacite and taenite. 7A and 7B are positions of the SIMS measurements.

acapulcoites cannot be produced by reduction of H-chondrite precursors followed by thermal metamorphism (Palme et al., 1981). Acapulcoites have conflicting properties. Although they are more equilibrated than type 6 ordinary chondrites yet they have higher contents of highly volatile elements including planetary rare gases (Palme et al., 1981; Schulz et al., 1982). The abundances of these elements decrease with increasing petrologic type, but are higher in Acapulcoites than in type 6 ordinary chondrites. This trend, contradicts the general accepted argument that higher equilibration temperatures, recorded in silicate mineral thermometers and based on textural evidence automatically leads to loss of volatiles, such as the sequence from type 3 to type 6 ordinary chondrites seem to imply. Following the type 3 to 6 trend carbon and nitrogen should be extremely depleted in Acapulco, but as we will show in this article, they are not. The mode of occurrence of carbon, siting of nitrogen and their isotopic compositions may reveal important clues to the formational history of acapulcoites, information not obtained from the study of the major silicates.

Meteorites from the acapulcoite-lodranite group have been subjected to comprehensive petrological, geochemical and isotopic investigations in an attempt to establish genetic links and differences between them and to resolve controversial conclusions concerning the thermal and cooling histories of their parent body (Palme et al., 1981; Schulz et al., 1982; Nagahara, 1992; Torigoye et al., 1993; Zipfel et al., 1995; Mittlefehldt et al., 1996; McCoy et al., 1996; McCoy et al., 1997a; McCoy et al., 1997b; Pellas et al., 1997; Floss, 2000; Min et al., 2003). It has been suggested that acapulcoites can be recognized from lodranites on the basis of the difference in their grain sizes. McCoy and coworkers reported that lodranites are coarse-grained whereas acapulcoites are fine-grained (McCoy et al., 1997a). They suggested that this dichotomy in grain size stems from a basic difference in their petrogenesis. Zipfel et al. (1995) emphasized that lodranites are depleted in elements that are enriched in early partial melts (e.g., Na, Al, LREE). Acapulcoites and some lodranites display a high degree of lithologic heterogeneity on a centimeter to millimeter scale (e.g., LEW 86220, McCoy et al., 1997b), a feature not observed in chondritic meteorites of petrologic type 6. This feature created considerable difficulties in understanding the petrologic and thermal histories of individual members of this group (Floss, 2000). There is general agreement that members of the acapulcoite-lodranite group originated from a chondritic asteroid of unique composition that has been subjected to a high-temperature metamorphic event. However, there is considerable disagreement concerning the peak temperatures, degree of partial melting, magnitude of melt migration, if any, and cooling rates of the various acapulcoites (Palme et al., 1981; Nagahara, 1992; Torigoye et al., 1993; Zipfel et al., 1995; Mittlefehldt et al., 1996; McCoy et al., 1996; McCoy et al., 1997a; McCoy et al., 1997b; Pellas et al., 1997; Min et al., 2003). An important feature of both acapulcoites and lodranites (except in LEW 86220) is the lack of any igneous texture indicative of total or partial melting followed by liquid-mineral crystallization as the latest event. Their texture is unequivocally indicative of solid-state recrystallization during a thermal metamorphic event leading to triple junctions. We caution, however, as we will show in this article that the lack of igneous texture does not negate that any member of this group was subjected to partial melting event before the final solid-state recrystallization took place.

The majority of the above-cited papers were devoted to investigations of silicate phase equilibria, metal compositions, phosphates, trace element abundances and isotopic dating systematics. Graphite, a very important accessory mineral, known for its high isotopic retentivity (El Goresy et al., 1995a; El Goresy et al., 1995b) has either been entirely ignored, or listed for mere mineralogical completeness, without further efforts to provide information on its morphologies, the isotopic compositions of carbon and nitrogen, or a discussion of the petrologic relevance of the graphite-bearing assemblages e.g., (Schulz et al., 1982; Nagahara, 1992). Recently, C- and N- isotopic compositions of graphite have been reported from the new lodranite Graves Nunatakes (Nittler and McCoy, 2000).

Little attention was also given to chromite-bearing mineral assemblages. No systematic studies of the chemical zoning of chromite in the different metal and silicate assemblages have been conducted. An exception is the report by (El Goresy and Janicke, 1995) on the zoning behavior of Acapulco chromites. This systematic study revealed four different populations of chromites with contrasting and complex chemical zoning trends. This is a clear evidence of lack of equilibration.

The Acapulco meteorite contains mineral constituents with distinct N-isotopic compositions. Previous investigations revealed contrasting N-isotopic signatures. While silicates (olivine, pyroxene, plagioclase) contain isotopically heavy nitrogen ($\delta^{15}N = +15‰$), chromites and metals have isotopically light nitrogen ($\delta^{15}N = -150$ to $-75‰$) (Sturgeon and Marti, 1991; Kim and Marti, 1994). In these studies no information has been given as to where the N is sited in the metal, whether totally in the metal, only in the graphite inclusions or in both.

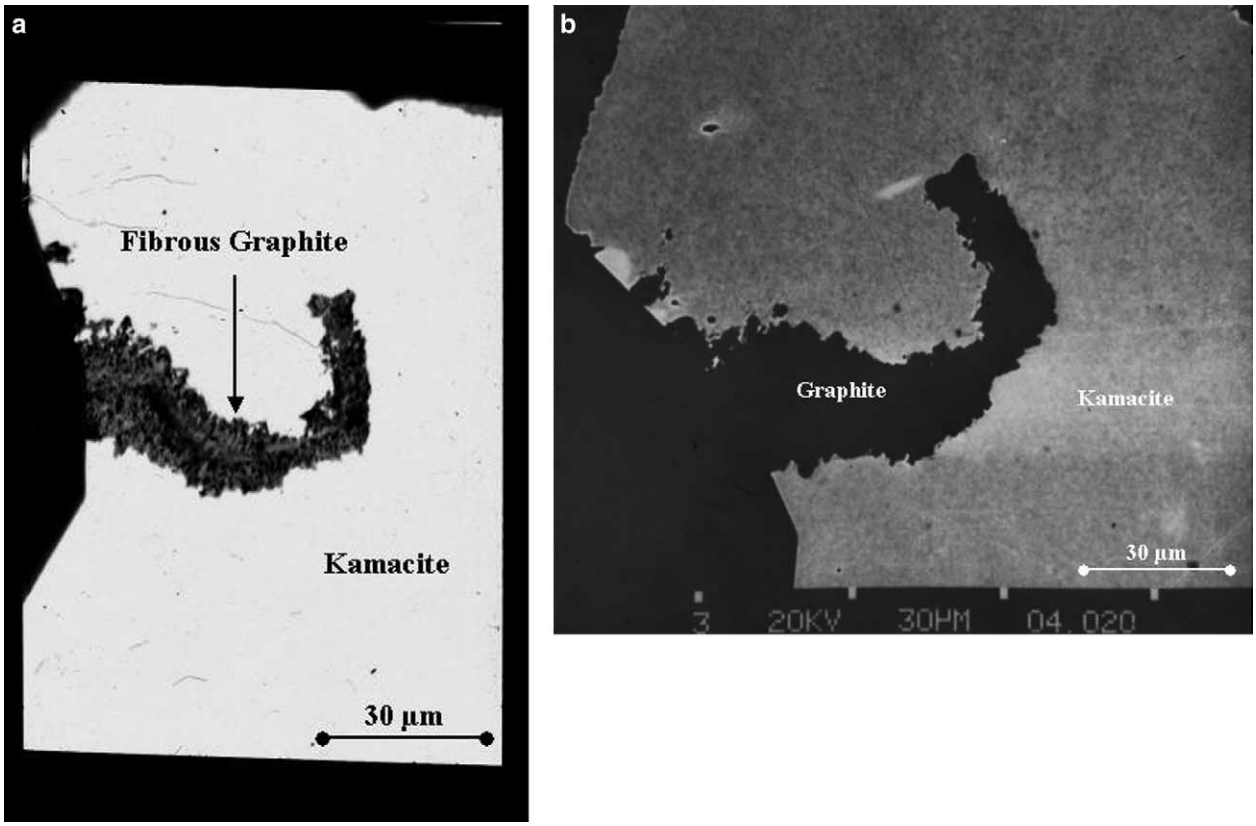

Fig. 2. (a) Reflected light microscopic photograph of a sickle-shaped band of fibrous graphite in kamacite. (b) back-scattered electron (BSE) photograph of the same region shown in (a), depicting the chemical homogeneity of the kamacite. Bright band in kamacite on the right hand site is due to charging.

An earlier combined petrographic and Secondary Ionization Mass Spectrometric (SIMS) investigation on Acapulco has indicated the presence of two graphite morphologies associated with metals with different carbon- and nitrogen-isotopic compositions: (1) spherulitic graphite with the $\delta^{13}C$ and $\delta^{15}N$ values plotting on a linear array with a slope of 3.25 in a $\delta^{13}C$ vs. $\delta^{15}N$ isotope diagram ($\delta^{13}C = -35$ to $-15‰$ and $\delta^{15}N = -142$ to $-67‰$), and (2) feathery graphite with the isotopic compositions: $\delta^{13}C = -20$ to $-8‰$ and $\delta^{15}N = -154$ to $-110‰$ (El Goresy et al., 1995a). We have expanded this combined study to additional samples of Acapulco to explore if the lithologic heterogeneity of this meteorite would reveal additional graphite morphologies with new isotopic signatures (El Goresy et al., 1995b). Further motivation for such a detailed study was provided by comprehensive petrographic and microprobe investigations on chemical zoning of chromites in Acapulco that revealed several contrasting zoning trends, thus indicating lack of equilibration during the thermal event in the region of the acapulcoite-lodranite parent body from which Acapulco originated (El Goresy and Janicke, 1995).

In this article, we report a detailed study of graphite in Acapulco. We focus on the morphology of graphite types, their mutual textural relations, their textural relations to kamacite and taenite, their C- and N-isotopic compositions and explore the possibility that morphologic differences and C- and N-isotopic signatures of the various graphite types reveal genetic clues to the evolution of the Acapulco parent body. We also present new data on the textural relations between kamacite, taenite and graphite. We report the occurrence of orthopyroxene-troilite symplectite, providing textural evidence for silicate-sulfide melting, and present textural evidence for the melting origin of the metal spherules in orthopyroxenes and olivines and discuss the previously reported Ni/Ir ratios (Zipfel et al., 1995) in matrix metal and in metal spherules in olivine and orthopyroxene. Furthermore, we evaluate the reliability of previously reported metallographic cooling rates in view of taenite-kamacite-graphite intergrowths encountered during this study. In addition, we discuss the contrasting models developed to explain the petrology as well as lithophile and siderophile trace element abundances of different minerals in acapulcoites.

2. ANALYTICAL METHODS

Four polished thin sections (PTS) of the Acapulco meteorite were investigated with reflected light microscopy and Scanning-Electron Microscopy (SEM) using back-scattered electron (BSE) imaging techniques. BSE imaging was used to delineate the textural relations of kamacite-taenite in conjunction with the origin of the metal-graphite and the Ni-diffusion characteristics at the kamacite-taenite boundaries. Carbon and nitrogen isotopic analyses of individual graphites were made on the PTS with the Washington University CAMECA IMS 3f ion microprobe following the procedures described by Zinner et al. (1989). A primary Cs^+ beam of ~2–3 μm in diameter was used to produce C^- and CN^- ions. The mass resolving power was sufficient (4500–5000) to separate $^{13}CH^-$ from $^{13}C^-$, $^{12}C^{15}N^-$ from $^{13}C^{14}N^-$, and $^{12}C^{14}N^-$ from $^{13}C^{13}CH^-$. Both C and N (via CN) were measured in the same analysis cycle. Analyses of Acapulco graphites were

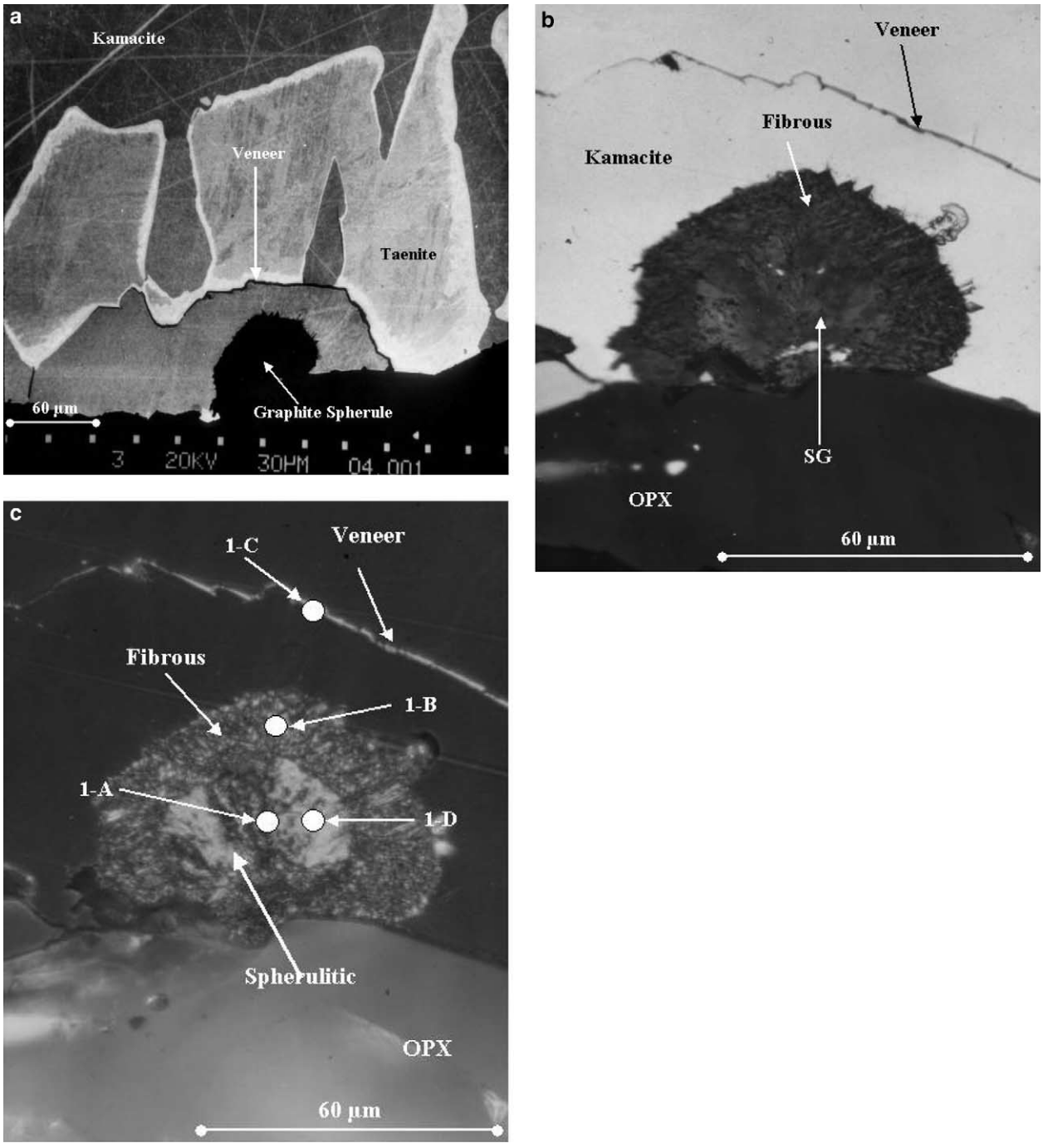

Fig. 3. (a) BSE photograph of a kamacite-taenite metal grain with various graphite morphologies (arrows). (b) Reflected light microscopic detail of the lower portion of the metal grain in (a), depicting the spherulitic graphite core (SG), the surrounding fibrous graphite band and the graphite veneer between kamacite and taenite. OPX is orthopyroxene (c) same photograph as in (b) but with crossed polars, depicting the sharp boundary between the spherulitic core and the fibrous graphite band as enhanced through anisotropism of graphite. Points 1A-1D are the positions of the SIMS measurements.

alternated with measurements of a laboratory carbon and nitrogen standard (colloidal graphite or DAG), having a well known isotopic composition, which had been deposited on the periphery of the sample mount. Measurements on the standards were used to determine the instrumental mass fractionation, which was applied to determine the true C and N isotopic ratios of the graphite grains.

Contamination is a potential problem during the nitrogen isotopic ratio measurements. It can arise from three different sources: exposure of the meteorite to the terrestrial environment, sample preparation, and nitrogen in the residual gas of the ion probe's sample chamber. Although N contamination in our analyses cannot be ruled out with absolute certainty, we believe it to be unlikely that the variations we observe in the N isotopic ratios are due to contamination. Acapulco, unlike acapulcoite and lodranite finds, is an observed fall. The degree

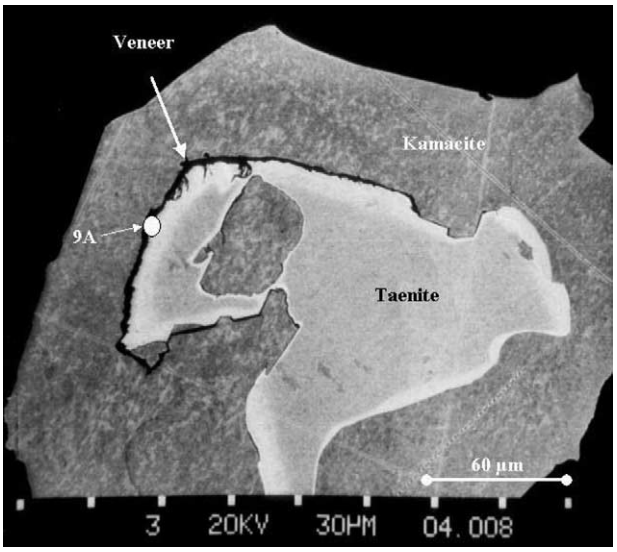

Fig. 4. BSE photograph of a bright taenite core completely surrounded by a polycrystalline kamacite rim. Taenite and kamacite are separated by a veneer of graphite (black narrow band). Point 9A is the position of the SIMS measurement.

of terrestrial weathering is small in comparison to other acapulcoite or lodranite finds. With only one exception (matrix graphite) we analyzed graphites that are enclosed in unweathered Fe-Ni metal grains. Extreme care was taken during sample preparation and polishing in the first place. In addition, only graphites whose metal hosts do not show any sign of weathering products at very high optical and SEM magnification were selected for SIMS analysis. During ion probe analysis the area to be analyzed was presputtered to remove the carbon coat and isotopic measurements were started when a constant CN^-/C^- ratio was achieved. Unless contamination from sample preparation penetrated in a uniform way into the graphite grains, these precautionary measures should have minimized contamination originating from sample preparation. Some degree of contamination from the residual gas in the sample chamber is unavoidable. The expected effect is that at very low intrinsic N concentrations contamination tends to pull the measured N isotopic ratios toward normal isotopic ratios (i.e., toward $\delta^{15}N = 0$). The data given in Appendix 2 indeed show that the highest $\delta^{15}N$ values are found in grains with the lowest CN^-/C^- ratios. However, the following arguments support our assumption that the N isotopic variations are intrinsic and that the effect of contamination must be much lower than these variations: (1) The negative correlation between $\delta^{15}N$ values and CN^-/C^- ratios does not hold any more if the results reported by El Goresy et al. (1995a) and shown in Appendix 1 are considered. Specifically, the last spherules in that table fall completely outside of this trend. (2) No correlation between the C and N isotopic ratios observed for spherulitic graphite (Figs. 15, 16) would be expected if the N isotopic variations were due to contamination. (3) During the C isotopic measurements of graphite in the iron meteorite San Juan reported by Maruoka et al. (2003) also N isotopic ratios were measured (unpublished data). In these analyses, made under the same instrumental conditions as for the Acapulco graphites, CN^-/C^- ratios ranged down to values of 3.5×10^{-4}, lower by a factor of five than those seen in Acapulco graphite. However, $\delta^{15}N$ values at these lowest ratios tend to be lower (more anomalous) than at higher ratios. Thus, the contamination contribution from the residual gas must correspond to an even smaller ratio than 3.5×10^{-4}. Even if we consider a potential contamination contribution to have this CN^-/C^- ratio and a normal N isotopic ratio, the calculated shift on isotopic ratios in Acapulco graphite with CN^-/C^- ratios of 2×10^{-3} and higher would be at most ~30‰.

3. RESULTS

3.1. Graphite Morphologies

The four PTS were scanned in detail in the reflected light microscope. Graphite morphologies in metal were also investigated in the SEM to explore any relationship between graphite settings and the diffusion behavior of Ni between kamacite and taenite. Graphite abundance in the four Acapulco sections is highly heterogeneous, demonstrating that the mineralogical heterogeneity is not restricted to chromite, phosphates and silicates (Palme et al., 1981, 1992; Zipfel et al., 1995; McCoy et al., 1996; McCoy et al., 1997a; McCoy et al., 1997b). A striking feature of the graphite rich metals is the paucity of cohenite. This mineral was observed only once as inclusion in a graphite-free metal grain not associated with any graphite (El Goresy et al., 1995a). More details about the genetic and carbon isotopic relevance of this observation will be said in the discussion in sections 4.1 and 4.2.

We have carefully screened the sections in search for thin metal or troilite veins cutting through cracks in mineral constituents and at grain boundaries everywhere in all sections (McCoy et al., 1996; McCoy et al., 1997a; McCoy et al., 1997b), to inspect if the veins are pristine to Acapulco or are genetically related to the fusion crust.

In addition to spherulitic (type 1) and feathery graphites (type 2) described before (El Goresy et al., 1995a), six additional types were encountered: (a) Round-, rectangular- or oval-shaped polycrystalline inclusions consisting of fine-grained graphite crystallites (crystallite size ~ 2 μm) in kamacite (type 3, Fig. 1). These do not have the radial structure of needle-shaped grains in common spherulitic objects described previously. The crystallites form triple junctions, which were produced through heating and solid-state recrystallization. Their presence may reveal important information about their parental carbon phase (see discussion section). (b) Bands (20–30 μm thick) of closely packed and parallel aligned fibrous graphite (type 4) occurring as individual inclusions in kamacite (Figs. 2a, b) or as tight rims around spherulitic graphite or the round, fine-grained spherules of types 1 and 3 (Fig. 3a–c). (c) Thin (< 10 μm) graphite veneers at the kamacite-taenite interface (type 5), probably formed by exsolution on cooling during the γ-α inversion (Figs. 3c and 4). The occurrence of these veneers has major implications for the application of metallographic cooling rate determination to the thermal history of Acapulco (see also next section and discussion). (d) Thin (<2 μm) graphite veneers between individual kamacite segments in composite metal grains (type 6, Fig. 5a, b). All veneers (types 5 and 6) consist of thin individual flat graphite crystals aligned in a trail along the kamacite-taenite boundary or between kamacite segments. Physical connections between spherulitic graphite and veneers are common so that it seems that graphite exsolution from metal during cooling may have grown onto preexisting graphite spherules and fine-grained objects (Fig. 6a, b and 7a, b). Different graphite morphologies abundantly occur together in the same metal grain. (e) Very small (1–3 μm) inclusions in some metal spherules (type 7, members of metal swarms) inside of orthopyroxene and olivine (Fig. 8). (f) Four single graphite crystals occurring in silicates but being attached to metal (type 8, Fig. 9a, b). Only one of these is majorly embed-

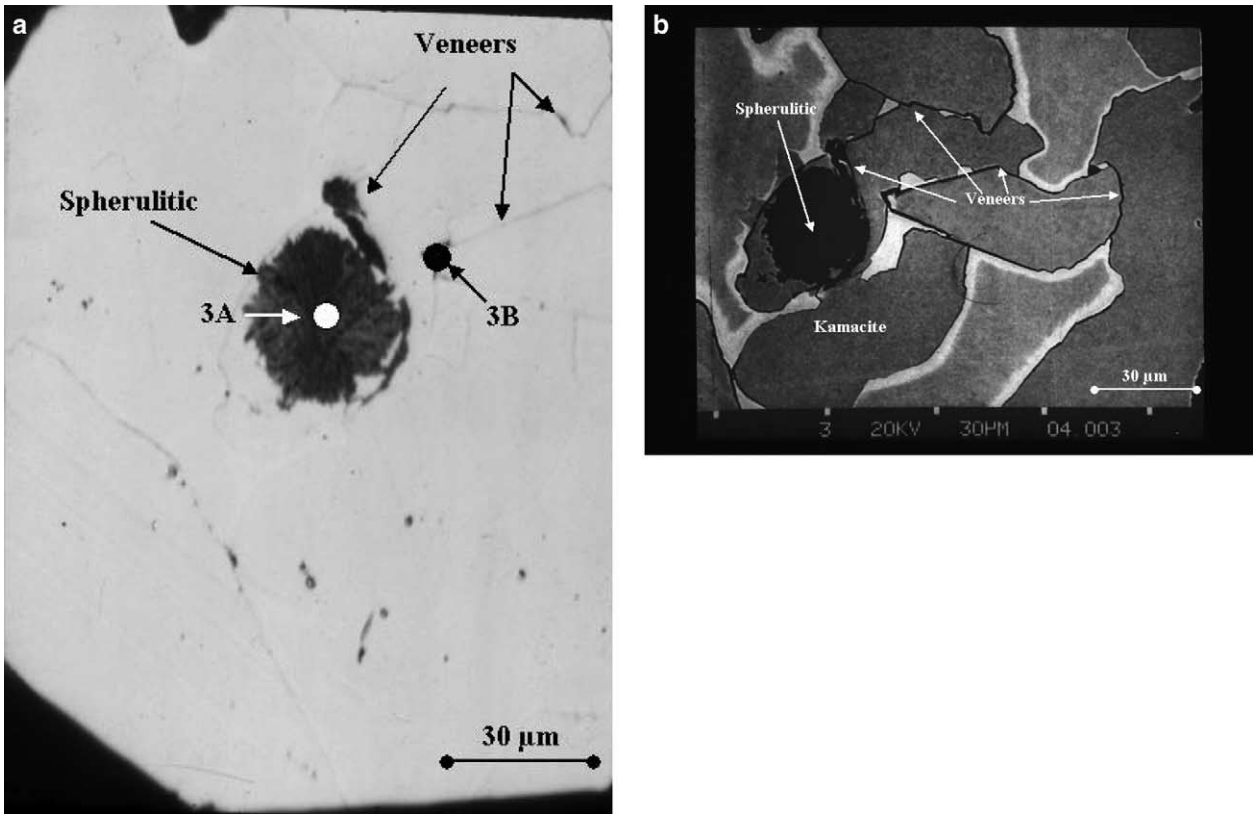

Fig. 5. (a) Reflected light microscopic photograph of a spherulitic graphite and exsolution graphite veneers in a polycrystalline kamacite-taenite grain Points 3A and 3B are positions of the SIMS measurements (b) BSE micrograph of the same area displaying kamacite segments (dark gray) and taenite (light gray with bright Ni-rich rims). Graphite veneers (black bands) separate kamacite from taenite and individual kamacite segments from each other.

ded in the matrix silicates but attached to two metal grains at small contact surfaces (Figs. 9a, b). The other three are intimately intergrown with FeNi metals with large contact surfaces.

3.2. Kamacite-Taenite and Metal-Graphite Textural Relations

As mentioned above, the majority of graphites are enclosed or associated with metallic FeNi grains. This raises two issues concerning their genesis: (1) are there any textural characteristics in the spatial intergrowths of graphite with kamacite and taenite? (2) Is there any tendency for particular graphite morphologies to occur in kamacite or in taenite? Kamacite and taenite always appear contiguous with each other. The former occurs in almost all metal grains studied as highly irregular bands partially or entirely surrounding taenite enclaves (Figs. 4a, 10a, b). Many taenite grains display a polycrystalline texture whereby a kamacite mantle surrounds several taenite enclaves. Surprisingly, this unique texture has only rarely been noticed before in any acapulcoite or lodranite (Palme et al., 1981; McCoy et al., 1996). Many grains, however, display plessite cores. Curved kamacite mantles surround both polycrystalline and homogeneous plessite cores (Fig. 11). This texture is, in contrast to those reported by Reisner and Goldstein in laboratory experiments and in ordinary chondrites (Reisner and Goldstein, 2003a; 2003b). The kamacite mantles are usually separated from the taenite cores by graphite veneers of various thicknesses (type 5). This important feature was first noticed by El Goresy and Zinner (1995b). In fact, the graphite veneers hermetically seal off both polycrystalline and homogeneous taenite enclaves from kamacite mantles and build diffusion barriers between kamacite and taenite. BSE imaging of taenite enclaves shows variations in brightness, indicating spatial heterogeneity of the Fe/Ni ratio. The polycrystalline taenite in some cases displays trellis-type lamellar structures with taenite fingers in a kamacite matrix, an intergrowth reminiscent of Widdmanstätten patterns (Palme et al., 1981) and martensitic texture (Fig. 11). In some cases kamacite mantles display a fine-grained polycrystalline texture. Like taenite cores, they are usually separated from each other by graphite veneers (Fig. 12a, b). All large graphite objects occur exclusively in kamacite. None of the different graphite morphologies display resorption at their boundaries to metal that could be suggestive of dissolution of carbon in the metal during the thermal history of Acapulco. Detailed metallographic information on the textures of polycrystalline and homogeneous metal grains will not be presented, since this needs a separate comprehensive treatment and is beyond the scope of this article.

All graphite types, except type 8, are either entirely enclosed in kamacite or attached to it. This puts stringent constraints to

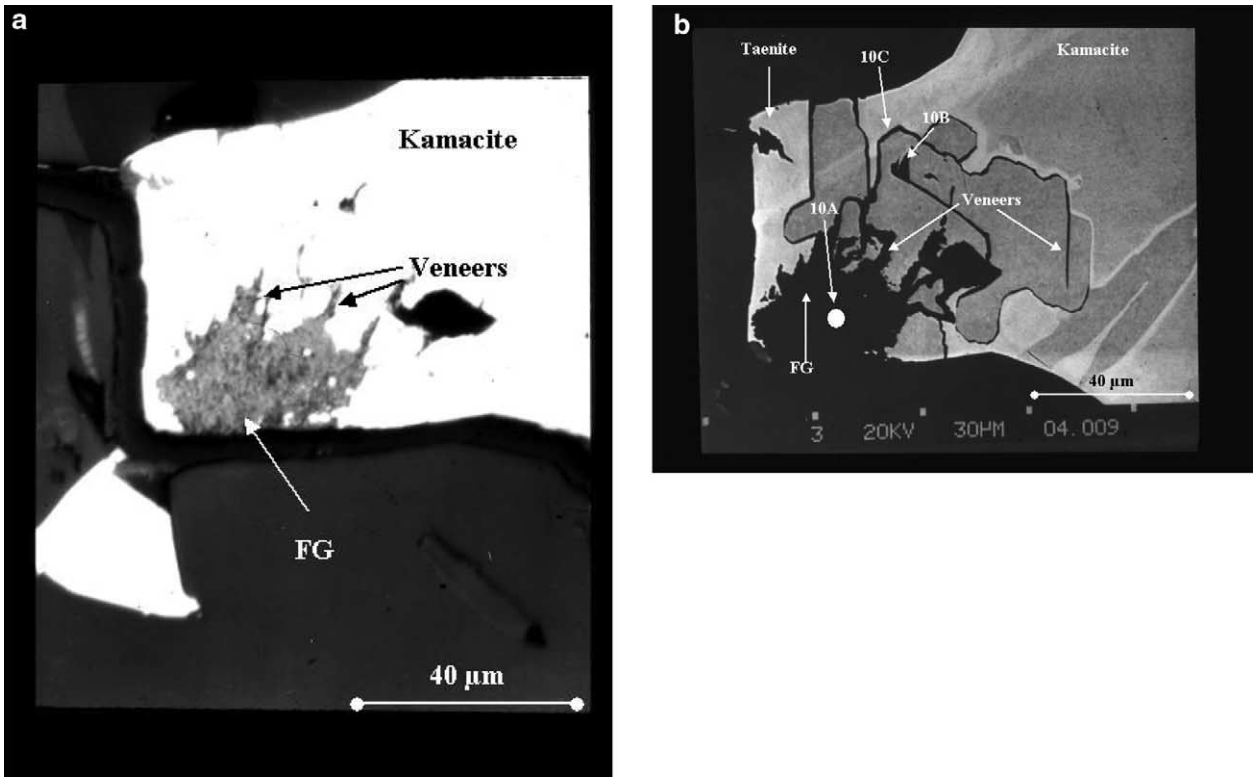

Fig. 6. (a) Reflected light micrograph of a fined-grained graphite (FG) inclusion in kamacite with branches of graphite veneers extending into the metal grain. (b) The same object in BSE image. This image also demonstrates that the graphite veneers hermetically separate taenite from kamacite Points 10A–10C are positions of the SIMS measurements.

their origin and interrelationship. Both types of graphite spherules (radial and polycrystalline fine grained) in kamacite must have predated the graphite exsolution veneers between kamacite and taenite and between individual kamacite grains, since in some cases the spherules apparently served as nucleation sites for the veneers whose growth originated at the surfaces of the spherules and extend deep into kamacite or between kamacite and taenite (Fig. 6a, b). Spherules must also have predated the fibrous bands (type 4) since the latter overgrew the spherulitic graphite (Fig. 6a, b).

Kamacite-taenite boundaries with graphite veneers or graphite of other morphologies display complex zoning textures. An example is shown in Figures 13a, b. While the kamacite mantles are chemically homogeneous and do not show any Ni depletion at the contact with the separating graphite veneer (Fig. 13b), the rims of the taenite cores in contact with the graphite consist of a fine structure of two successive thin layers with different brightness signaling different Ni-contents: (1) a polycrystalline innermost layer <6 μm in thickness, perhaps of martensitic nature, and (2) a darker ~ 2 μm wide Ni-poor layer (6.9 wt % Ni) in contact with the inner surface of the graphite veneer with BSE brightness slightly brighter than kamacite i.e., slightly higher in Ni than the latter. These textures demonstrate that Ni diffusion between kamacite mantles and taenite cores of the metal grains was impeded by the growing graphite barrier and ceased at some stage during cooling of the Acapulco meteorite and during graphite exsolution. This resulted in the exsolution of a new thin kamacite layer behind the graphite diffusion veneer barrier. We also encounter textures suggestive of growth of minute pin-shaped graphite crystals (less than 5 μm in length) from preexisting fine-grained graphite into kamacite, whereas graphite adjacent to plessite is smooth without such growth features (Fig. 7a, b). Although the origin of these pin-shaped crystals is not clear, it is possible that they also formed during cooling by exsolution from kamacite.

3.3. Carbon and Nitrogen Isotopic Compositions

Carbon and nitrogen isotopic compositions of all graphite type analyzed are given in Appendices 1 and 2 and plotted in Figures 14–16. Appendix 1 contains the data previously reported by El Goresy et al. (1995a) whereas Appendix 2 contains new analyses. Our new measurements reveal diverse C- and N- isotopic compositions in the different morphologies, with variations being much larger than those previously found in spherulitic and feathery graphites (El Goresy et al., 1995a). Figure 14 displays the $\delta^{13}C$ vs. $\delta^{15}N$ ratios of graphites shown in Figure 3c. Plotted in the same diagram are the previously determined isotopic compositions of spherulitic graphites for comparison (El Goresy et al., 1995a). Two measurements in spherulitic graphite (points Graph-1-A.1 and Graph-1-D.1 in Fig. 3c and Appendix 2) have $\delta^{13}C$ -11.1 ± 2.7‰ and $\delta^{15}N = -72.0 \pm 22.3$‰, and $\delta^{13}C = -11.9 \pm 2.6$‰ and $\delta^{15}N = -69.9 \pm 24.5$‰, respectively (Fig. 14). The 15 μm wide band of fibrous graphite surrounding the graphite spherule (Fig. 3c) has a C-isotopic composition similar to that of the spheru-

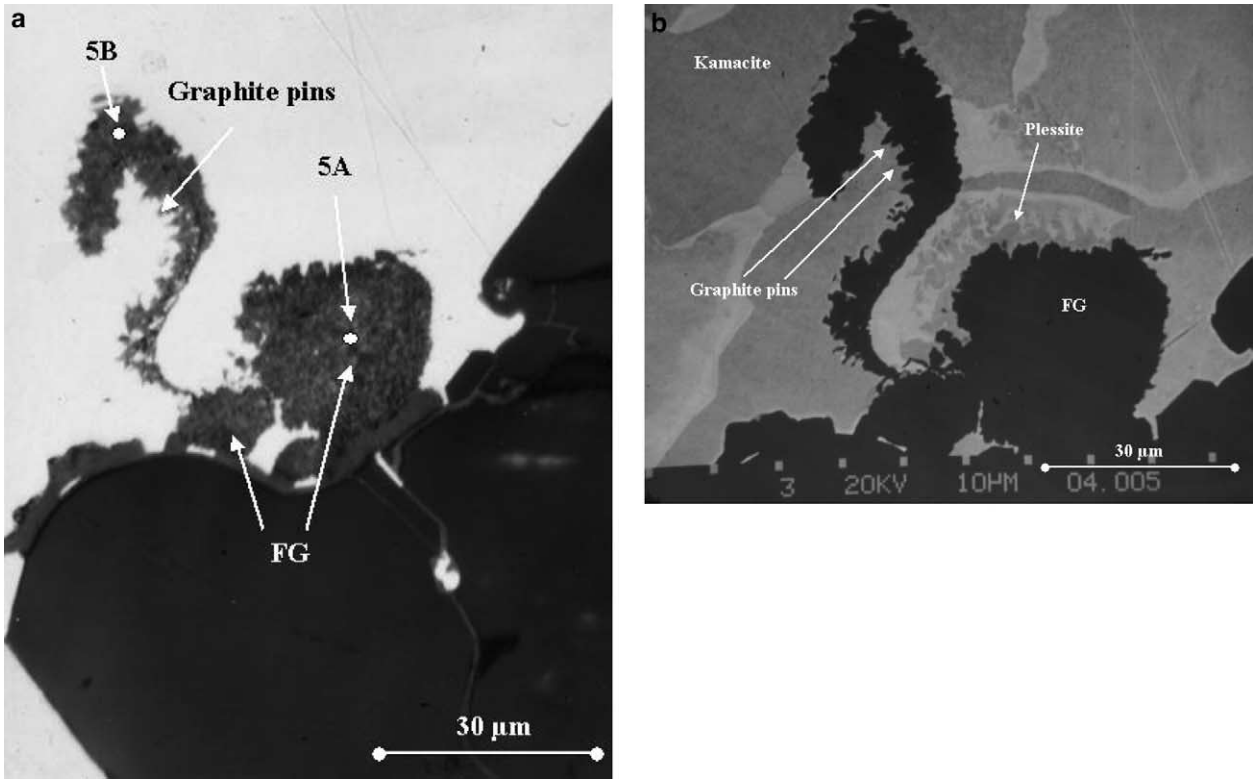

Fig. 7. (a) Reflected light photomicrograph of different graphite morphologies enclosed in FeNi metal showing two fine-grained spherulitic graphites(FG) near the edge of the metal grain and a sickle-shaped branch of graphite. Well developed graphite pins. Points 5A and 5B are positions of the SIMS measurements (b) BSE micrograph of same object as in (a) closely resolving the polycrystalline nature of taenite outside of the graphite sickle and the well developed graphite pins on the interior side of the graphite sickle bordering kamacite.

litic core, but isotopically much lighter N ($\delta^{13}C = -11 \pm 2.7‰$ and $-9.5 \pm 2.6‰$; $\delta^{15}N = -148.0 \pm 11.4‰$ and $-143.5 \pm 9.8‰$, respectively) (Appendix 2 and Fig. 14). In contrast, the graphite veneer between kamacite and taenite, located only 20 μm away from the fibrous graphite, has isotopically much lighter C and N ($\delta^{13}C = -18.5 \pm 2.9‰$ and $\delta^{15}N = -159.0 \pm 12.6‰$), (Appendix 2 and Fig. 14). Figure 15 displays the C- and N-isotopic compositions (GRAPH-3-A&B and GRAPH-21-A&C in Appendix 2) of two spherulitic graphites shown in Figures 5a, b, and 11a, b, respectively of the graphite veneers in two of the host metal grains, and, for comparison, of one matrix graphite. The isotopic compositions of the graphite spherules and the exsolution veneers are similar ($\delta^{13}C = -17.5 \pm 2.5‰$ to $-21. \pm 3.1‰$ and $\delta^{15}N = -141.3 \pm 19.5‰$ to $-154.9 \pm 8.5‰$). In contrast, the matrix graphite has isotopically heavy carbon and has heavier nitrogen than the exsolution veneers ($\delta^{13}C = 14.3 \pm 2.4‰$ and $\delta^{15}N = -103.4 \pm 10.9‰$). The isotopic ratios of various graphites plotted in Figures 14–15 demonstrate the diversity of the isotopic compositions as a function of morphology and the assemblage in which the graphite grains occur. Figure 16 shows the C- and N-isotopic compositions of all graphite morphologies studied. Four isotopically different populations can be recognized in this plot: (1) spherulitic graphite whose data points plot along an array of slope 3.25, extrapolating close to zero $\delta^{13}C$ and $\delta^{15}N$ values (El Goresy et al., 1995a); (2) graphite exsolutions with isotopically very light nitrogen; (3) feathery graphite and fine-grained spherules; and (4) one matrix graphite crystal with isotopically heavy carbon. The exsolution veneers have the lightest N-isotopic compositions, whereas the matrix graphite has the heaviest carbon, differing in $\delta^{13}C$ by 38‰ from the

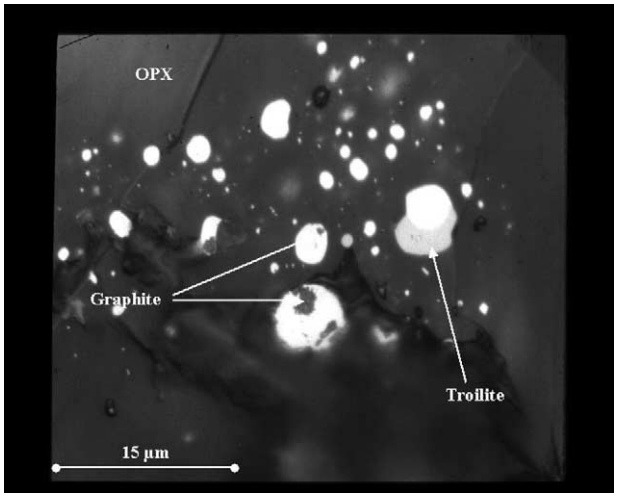

Fig. 8. A reflected light microscopic photograph depicting metal spherules enclosed in orthopyroxene. Three of these metal spherules contain small graphite inclusions. SIMS analyses were conducted on the largest of these graphites in the largest metal grain.

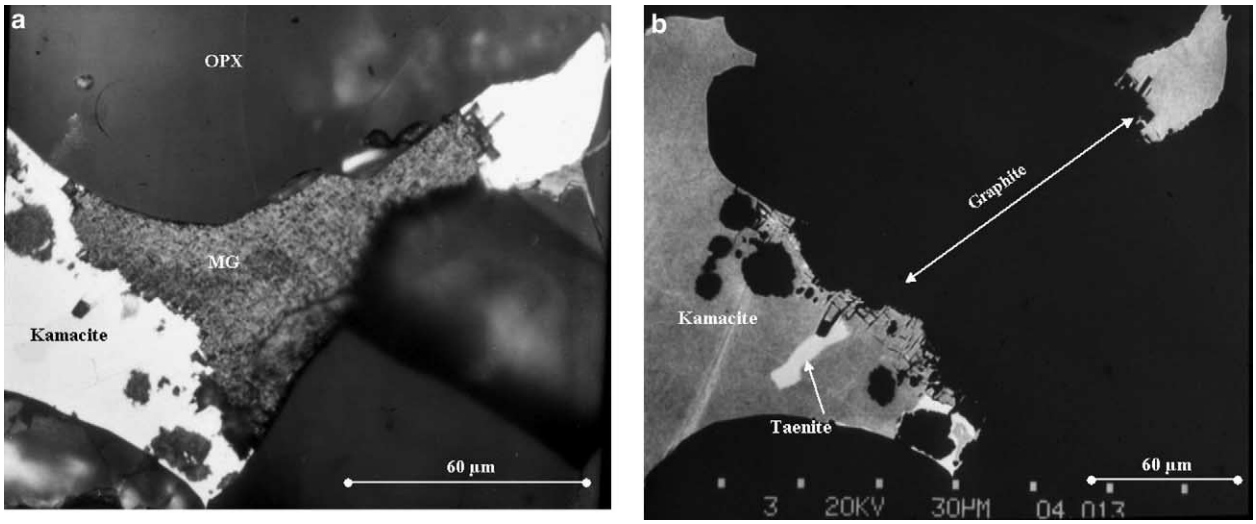

Fig. 9. (a) Reflected light micrograph of a single graphite crystal in the silicate matrix (MG) but attached at both ends to metal grains and several graphite spherules in the left metal grain. (b) BSE image of the same object. The graphite is here invisible due to very low brightness. The metal grains exhibit box-structure-like graphite exsolution (arrows adjacent to the matrix graphite crystal).

exsolutions. A graphite in a metal spherule inside orthopyroxene has $\delta^{13}C = -2.9 \pm 2.5‰$ and $\delta^{15}N = -101.2 \pm 32‰$. Its composition lies close to those of fine-grained spherules, rims, and feathery graphite (El Goresy et al., 1995a), however at the C-heavy end of this cluster. This suggests a genetic link between this graphite, the feathery graphite and fine-grained graphite spherules. The relevance of these isotopic differences and similarities will be discussed in the next section.

4. DISCUSSION

The here presented textural relations of graphites and their isotopic characteristics contain genetically important information that allows shedding light on the complex evolutionary history of the Acapulco meteorite back to its preaccretionary time. We address here several points that may clarify controversies on the evolution of Acapulco and perhaps other acapulcoites: (1) graphite morphologies and their possible formation processes; (2) textural relations of graphite exsolution veneers between kamacite and taenite and implications for obtaining meaningful metallographic cooling rates; (3) orientation of metal-troilite spherules in cores of orthopyroxenes and olivines, and the construction of a plausible formation model in comparison with other interpretations (Mittlefehldt et al., 1996; McCoy et al., 1996; McCoy et al., 1997b) and interpretations deduced from disequilibrium melting experiments on the Leedey L6 chondrite (Feldstein et al., 2001); (4) troilite-or-

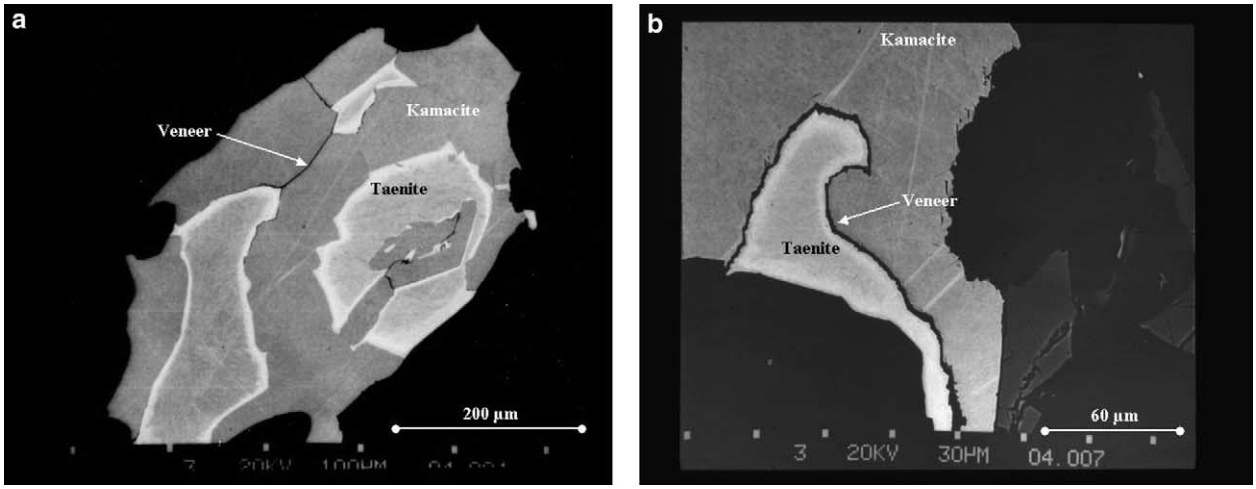

Fig. 10. (a) BSE photograph of a composite kamacite-taenite metal grain. The kamacite mantle (gray) surrounds several taenite enclaves. Graphite exsolution veneers separating kamacite and taenite segments (black bands) are present. (b) BSE photogreaph of a kamacite-taenite metal grain with curved contact along which an exsolution graphite veneer (black band) formed.

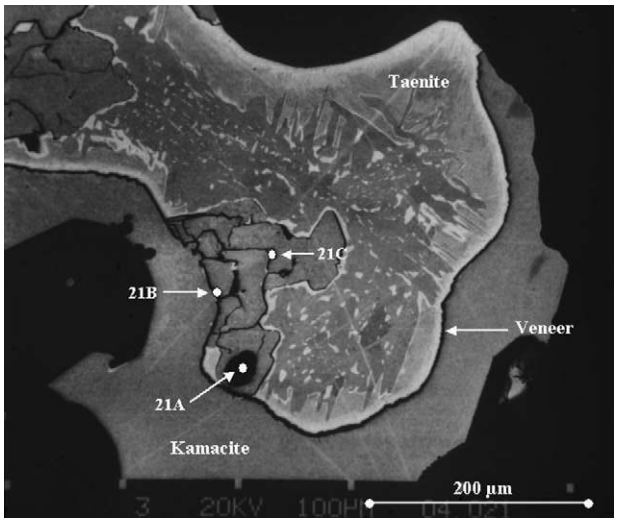

Fig. 11. BSE image of kamacite-taenite composite grain. Kamacite rimming the taenite interior is hermetically separated from the taenite by a continuous graphite veneer (black band). Graphite bands also separate the different kamacite segments (center). A graphite spherule is enclosed in kamacite (arrow). The taenite interior displays Widdmannstätten-like lamellar patterns. Points 21A–21C are positions of the SIMS measurements.

thopyroxene and chromite-orthopyroxene symplectites, subsequently first discovered in this study in Acapulco and in other new Antarctic acapulcoites; (5) Ir/Ni ratios of metal spherules in comparison to those of metals in chondrules (Grossman and Wasson, 1985; Zipfel et al., 1995); (6) troilite veinlets and metal patches and their relevance to the proposed melt migration model (McCoy et al., 1996; McCoy et al., 1997b); and (7) C- and N-isotopic compositions of graphite morphologies in Acapulco and one lodranite and their relevance to the evolution of their parent body.

4.1. Possible Formation Processes of Graphite Morphologies

Graphite in acapulcoites and lodranites seems to be rare. However, when present, its spatial distribution is heterogeneous in both meteorite subclasses. Notwithstanding the heterogeneous distribution, its presence may reveal important information on the preaccretionary history of these meteorites. The diversity of different graphite morphologies in Acapulco, even within only tens of microns distance, in the same metal grain, clearly indicates different processes of graphite formation. In situ formation of the different graphite morphologies by breakdown of preexiting cohenite can be ruled out, because it was experimentally demonstrated that breakdown of cohenite leads to the formation of cliftonitic graphite and Ni-poor kamacite (Brett and Higgins, 1967). It may appear surprising, that none of the graphite morphologies display a cohenite belt at the graphite-metal interface. Mass balance estimates of the graphite-rich metal grains indicate that a carbon-content in excess of 0.5 wt. % in solid solution in metal is required, should all graphite morphologies have exsolved from an Fe-Ni-C alloy at T >700°C. Acapulco metal contains 9.00 and 9.9 wt. Ni (Palme et al., 1981). Such carbon and nickel contents would place the bulk metal composition in the $\alpha + \gamma +$ cohenite field above 650°C (Brett, 1967). This would have inevitably resulted in the crystallization of cohenite belts around every graphite morphology and subsequently the formation of cliftonitic graphite and Ni-poor kamacite upon breakdown of cohenite. El Goresy et al., (1995a) reported a small cohenite speck in a metal grain in Acapulco that depicts no signs of breakdown. Neither cliftonitic graphite, nor a secondary Ni-poor (< 1 wt. % Ni) kamacite were encountered in any of the metals in the studied sections. For this reason we argue that the carbon content of the metals were definitely below 0.5 wt. % and that the graphite morphologies didn't exsolve from a carbon-rich metal alloy, thus placing the metal bulk compositions in the γ or the $\alpha + \gamma$ fields below 723°C (Brett, 1967). For more details of the phase relations see isothermal sections of the system Fe-Ni-C of (Brett, 1967). Consequently, with the exception of the graphite veneers between kamacite and taenite, and graphite specks in metal spherules in orthopyroxene and olivine, the different graphite morphologies cannot have in situ exsolved from a carbon rich Fe-Ni-C alloy in their metal hosts, or in the silicate matrix in the Acapulco meteorite (or its parent body). We cannot entirely exclude the possibility that a small part of the primary graphite dissolved in the metal at high temperatures. At any case, the lack of cohenite and its breakdown products, the lack of reaction textures between metal and graphite, and specifically, the carbon isotopic compositions of the graphite veneers argue against in situ formation of the graphite morphologies by exsolution from a carbon-rich metal alloy. Very fast cooling (Min et al., 2003) must have inhibited massive dissolution of graphite in the metal alloy. In contrast, graphite veneers must have exsolved in situ from their parental C-bearing metals in the course of the γ-α inversion of metallic FeNi during cooling of Acapulco in its parent body. With the exception of graphite inclusions in metal spherules in the cores of orthopyroxenes and olivines and of graphite veneers all other graphite types were very probably captured during growth of the individual metal grains *prior* to the accretion of Acapulco's primordial constituents in the parent body. The growth of the individual different morphologies probably took place in different reservoirs at different temperatures and condensation rates before their inclusion in their common metal hosts. The in situ growth in individual metal grains during the heating event that Acapulco experienced and subsequent cooling in the parent body would have produced many graphite grains with the same morphology, and with identical carbon and nitrogen isotopic signatures. In addition, in situ growth would have resulted in homogeneous abundance of graphites in the majority of, if not all, metal grains. This, however, is not the case (see above). The diversity of the morphologies strongly hints to different preaccretionary formation conditions (perhaps in different reservoirs) and subsequent heterogeneous incorporation into condensing FeNi metal grains. Growth conditions probably changed several times before accretion, since we encounter overgrowths of different morphologies, e.g., bands of fibrous graphite around spherulitic graphite, both differing in their N isotopic compositions (Figs. 3a–c and 14). The heterogeneous distributions of the graphite morphologies in metals and the variety of morphologic types enclosed in individual metal grains argue for a heterogeneous mix of graphite types during growth of the metal grains. If our interpretation is correct, then the graphites must bear preaccre-

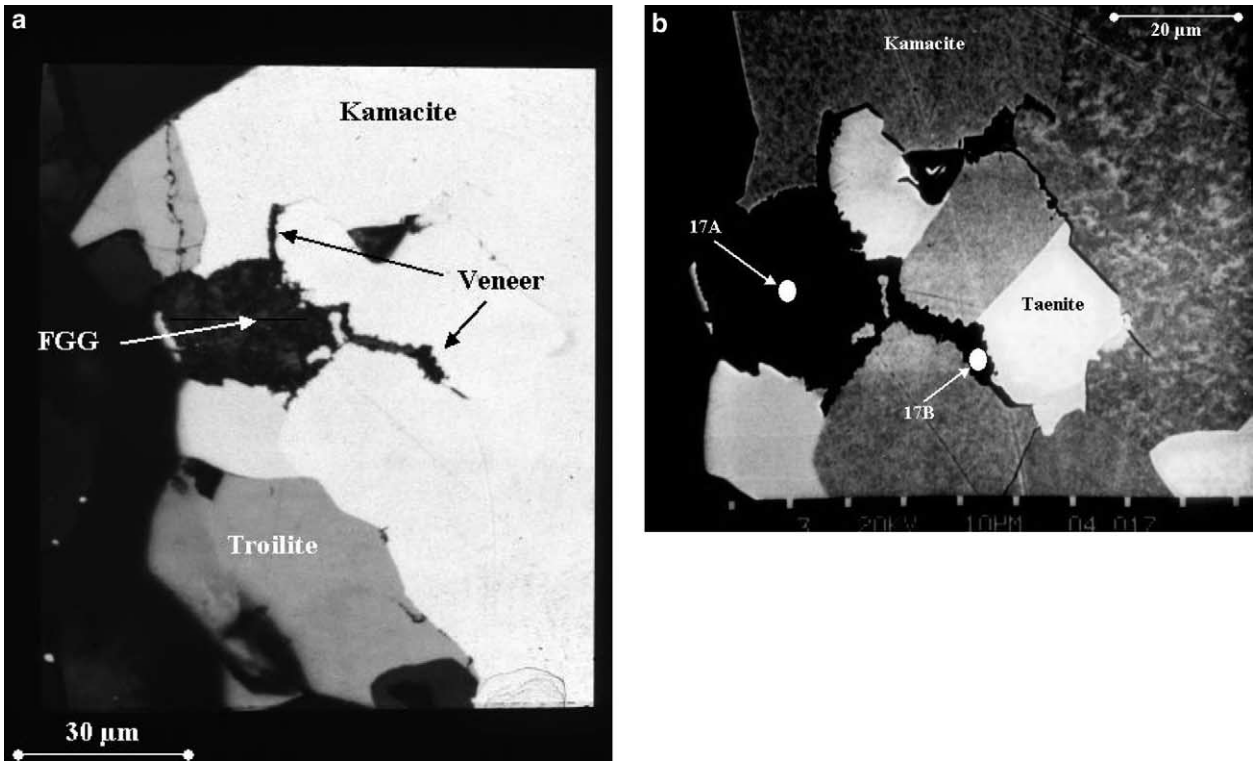

Fig. 12. (a) Reflected light photomicrograph showing a graphite fine-grained spherule (FGG) in kamacite attached to two branches of exsolution graphite veneers. (b) BSE image of same area shown in (a). The graphite spherule and the exsolution branches attached to it occur between kamacite and taenite and between individual kamacite segments (arrows). Kamacite displays both homogeneous and polycrystalline features in different segments. Points 17A–17B are positions of the SIMS measurements

tionary signatures that were not overprinted during the heating and rapid cooling of the Acapulco parent body. Spherulitic graphite has previously been reported from the acapulcoite ALH 77081 (Schulz et al., 1982) and uncharacterized graphite types from the acapulcoite Yamato-8002 (Nagahara, 1992), however no isotopic data of these graphites have been published from these acapulcoites. Unfortunately, no further information on graphite abundances and distribution in other acapulcoites is available. High graphite abundances were recently found in three new Antarctic acapulcoites (Nakamura et al., 2005).

Spherulitic graphite has been previously reported from silicate-rich enclaves in terrestrial sulfide deposits, however no information about their formation conditions has been given (Ramdohr, 1980). Centimeter-long needle-shaped trigonal crystals of graphite, similar to the individual acicular forms described here, have previously been reported by Ramdohr from the Mundrabilla meteorite (Ramdohr, 1980). However, little can be said here about the physico-chemical conditions leading to the menagerie of graphite morphologies encountered in Acapulco, since to the best of our knowledge the origin of growth textures of graphites has been not adequately explored in laboratory experiments. The texture of the oval or rectangular polycrystalline graphite may have been produced by recrystallization of another metastable carbon form or of poorly graphitized carbon during the heating event of Acapulco. This interpretation is supported by the occurrence of triple junctions between the individual graphite crystallites. We envisage that this polycrystalline graphite recrystallized from either primary amorphous or poorly graphitized carbon in the Acapulco parent body during heating in its early history. Finally, a recent microscopic scrutiny of four sections of the Monument Draw acapulcoite revealed that metal patches, metal grains and the silicate matrix are barren of graphite (Chen and El Goresy, 2005).

Individual graphite "rosettes" were recently found in the lodranite Graves Nunataks (Nittler and McCoy, 2000; Stroud et al., 2001). These authors report millimeter-sized graphite "rosettes" (presumably spherulitic graphite) within α FeNi metal sheets, whereas other "rosettes" in the matrix metals are much smaller ($\sim$ 400 μm). Three graphite "rosettes" were analyzed by SIMS for their nitrogen and carbon isotopic compositions. All "rosettes" are extremely poor in nitrogen, which is isotopically normal (Nittler and McCoy, 2000). The carbon and nitrogen isotopic compositions of the "rosettes" in the two different metal types are difficult to understand in the context of the offered models (Nittler and McCoy, 2000). More about this will be said in the discussion of the graphite's isotopic compositions. We consider the apparent non-uniform distribution of graphite in meteorites of the acapulcoite-lodranite family as ample evidence for heterogeneous accretion of graphite and metals in the source accretion. This heterogeneity during the accretion of the acapulcoite-lodranite parent body was not restricted to metals and graphite, but also included chromite,

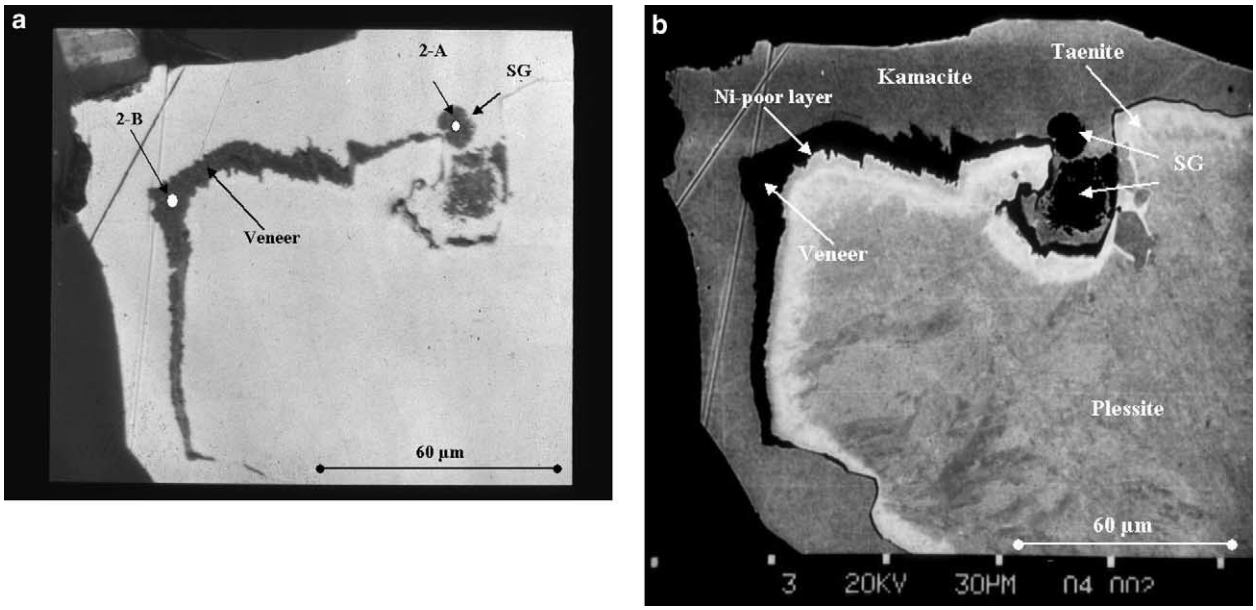

Fig. 13. (a) Reflected light micrograph of a large metal grain with a graphite spherule and a thick graphite veneer between kamacite and taenite. Points 2A and 2B are positions of the SIMS measurements (b) BSE photograph of the same area, depicting the complete separation of the homogeneous kamcite rim from the heterogeneous taenite core. The multizoned metal layer with a Ni-poor layer next to the graphite veneer is visible.

phosphates and perhaps silicates as previously pointed out by (Mittlefehldt et al., 1996). This calls for caution in interpreting the genetic relevance of the abundances of the lithophile and siderophile elements in members of this group.

Spherulitic and feathery graphite morphologies were recently also reported from unequilibrated ordinary and carbonaceous chondrites (Mostefaoui et al., 2005). Formation of these two morphologies was evidently not restricted to the region of the solar nebula from which Acapulco-type meteorites originated. However, the assemblages in which the different graphite morphologies occur in chondrites are not restricted to metallic FeNi metal spherules or sheets as they are in acapulcoites and one lodranite. Many textures and graphite associations in ordinary chondrites are distinctly different from those in acapulcoites and lodranites. Some of the graphites in these meteorites have isotopic signatures that have been interpreted to be of interstellar origin (Mostefaoui et al., 2005), however others, though preaccretionary, may have suffered from overprinting of their nature and isotopic compositions in their parent bodies (Mostefaoui et al., 2005).

4.2. Textural Relations of Exsolution Veneers Between Kamacite and Taenite and the Problem of Obtaining Correct Metallographic Cooling Rates

An important prerequisite for the determination of metallographic cooling rates based on Ni-concentration profiles in metal grains is the unimpeded Ni diffusion between kamacite and taenite having formed from a phosphorous-free FeNi system. However, Acapulco metals have graphite barriers between kamacite and taenite that exsolved from taenite during the γ-α inversion at sometime during the cooling of Acapulco at T $<$723°C (see details in section 4.1). These graphite barriers heavily impeded or entirely inhibited any Ni interdiffusion after their formation. Figure 13b depicts a Ni-poor layer at the inner surface of the graphite veneer, indicating its formation after the exsolution of graphite because it blocked Fe-diffusion from taenite to the outer kamacite layer. McCoy et al. (1996) suggest that these graphite veneers likely formed at temperatures below that at which the taenite composition was established. However, these authors did not present any evidence supporting this claim. Fe diffusion to kamacite and Ni diffusion from kamacite to taenite was active but only until the boundary between the two metals was sealed off by the graphite barrier, thus leading to the formation of a new kamacite layer behind the graphite

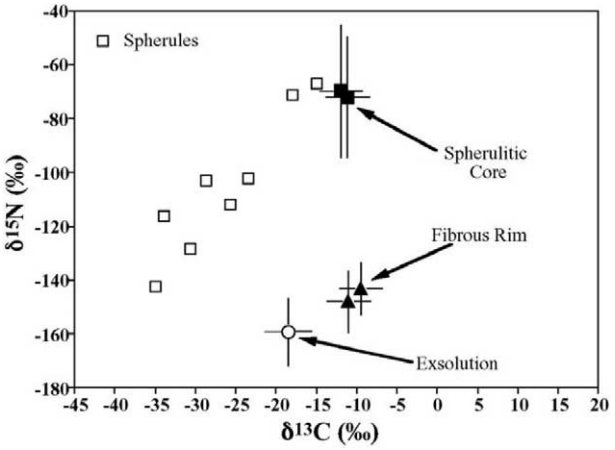

Fig. 14. A δ^{15}N vs. δ^{13}C isotope plot of various spherulitic graphites, the core and surrounding fibrous graphite of the graphite spherule and the exsolution veneer between kamacite and taenite depicted in Figure 3b.

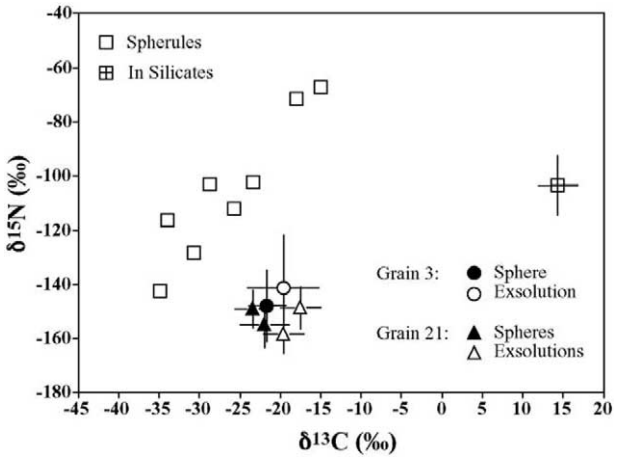

Fig. 15. A $\delta^{15}N$ vs. $\delta^{13}C$ isotope plot of the two spherulitic graphites shown in Figures 5a and b and 11, respectively, the overgrown graphite veneers in the two in host metal grains and, for comparison, the isotopic compositions of one matrix graphite.

veneer (Fig. 13b). We argue that the measurement of Ni profiles at the edge of taenite grains in Acapulco cannot lead to meaningful cooling rates. In fact, Figure 6c of McCoy et al. (1996) does not give any reliable estimates on the metallographic cooling rates of Acapulco. Another problem is that metals in Acapulco contain considerable amounts of phosphorus and silicon (up to 700 ppm phosphorous and 300 ppm silicon respectively (Pack et al., 2005)) that makes the metallographic cooling rate technique inapplicable (Reisner and Goldstein, 2003a; 2003b). In contrast, the calculated cooling rates for ALH 81261 and Monument Draw (McCoy et al., 1996) may be reliable, because no graphite barriers were encountered in the metals of Monument Draw (Chen and El Goresy, 2005), but provided that these metals are phosphorous free (Reisner and Goldstein, 2003a; 2003b).

4.3. Orientation of Metal-Troilite Spherules in Cores of Orthopyroxenes and Olivines

The mode of occurrence of metal-sulfide spherules in Acapulco and their possible origin has been debated and several contradictory formation mechanisms have been offered (Palme et al., 1981; Zipfel et al., 1995; Mittlefehldt et al., 1996; McCoy et al., 1996; McCoy et al., 1997a; McCoy et al., 1997b; Feldstein et al., 2001). Palme et al. (1981) and Zipfel et al. (1995) were the first who observed that the spherules usually occur in the cores of orthopyroxenes and are less abundant in olivine cores. They proposed that the spherules had been deposited during early partial melting of Acapulco on the surfaces of residual orthopyroxene and olivine grains and were trapped during further growth of these grains from the silicate melt. Major constituents of the spherules are FeNi metal and troilite. Metal spherules in Acapulco consist of FeNi metal (average Ni-content 8%), in some cases they have graphite inclusions and phosphates attached to their edges. Troilite spherules are majorly monomineralic. A careful scanning of the metal-troilite spherules in the present study both in reflected light and SEM revealed no chromite inclusions. Metal spherules in semicircular arrangements in the core of a single olivine grain in ALH 77081(Figure 1 in Schulz et al., 1982) were incorrectly interpreted as outlining contours of preexisting chondrules (Schulz et al., 1982). Unfortunately, this incorrect interpretation has been adopted by some authors, which led to considerable confusion and the claim that the arrangement of the metal spherules represents a texture inherited from preexisting chondrules (Mittlefehldt et al., 1996). To the best of our knowledge no such concentrically decorated metal or sulfide spherules in individual silicate crystals have ever been reported from chondrules in any chondrite regardless of chondrite class and degree of equilibration. Metal spherules in dusty olivines in some chondrites have a heterogeneous, entirely different, distribution within olivine grains. In addition, they are depleted in Ni since they were produced during reduction of parental Fe-rich olivines.

Mittlefehldt et al. (1996) correctly reasoned that the inclusions should decorate the former grain boundaries of solid residual silicates, if the mode of formation proposed by Palme et al. (1981) and Zipfel et al. (1995) is correct. However, Mittlefehldt et al. (1996) incorrectly claim that the metal spherules in Acapulco are randomly distributed throughout the cores of some olivine and orthopyroxene grains.

We emphasize that a correct determination of the abundance and decoration of metal-sulfide spherules can be obtained only with three-dimensional optical tomography in reflected light microscopy at and below the polished section surface. This approach can determine whether there is a decorative arrangement of metal spherules around an orthopyroxene or olivine core, or a mere random cluster in these cores as claimed by Mittlefehldt et al. (1996). SEM studies alone cannot reveal any information on the orientation of the spherules if they are decorating an orthopyroxene core of an individual crystal, since the investigations are restricted to the polished surface whose spatial sectioning position, if through the metal swarm above or below the orthopyroxene core or across the metal free core and the decorating swarm, is unknown. We emphasize that not each orthopyroxene or olivine grain containing spherules would display the expected decorative pattern at the polished section surface, since such decoration features can only be visible in

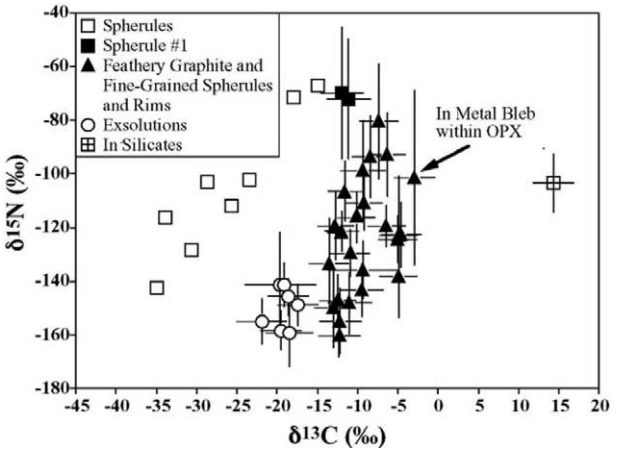

Fig. 16. A $\delta^{15}N$ vs. $\delta^{13}C$ isotope plot of all graphite morphologies analyzed in the Acapulco samples.

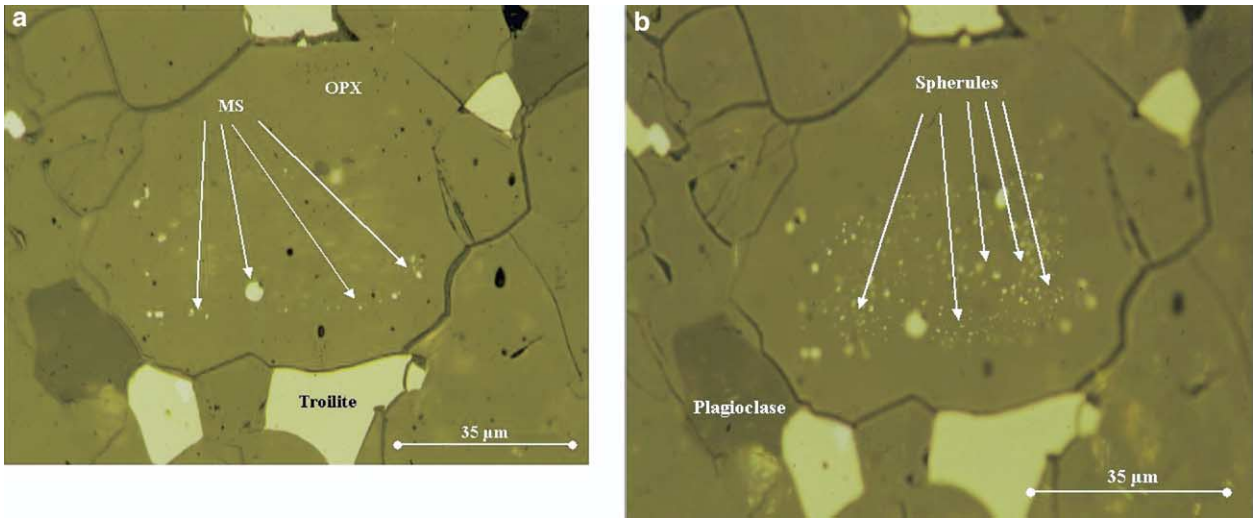

Fig. 17. (a) Reflected light micrograph of an orthopyroxene grain whose core is decorated with metal spherules (MS, arrows). Microscope focused at the section surface. (b) Picture of the same grain as in (a) with microscope focused on the metal spherule envelope below the polished surface in the interior of the orthopyroxene.

grains sectioned through their cores. Olivines and orthopyroxens do not have a preferable fabric in any acapulcoite or lodranite. Hence, these grains will be sectioned randomly at different positions: through the metal free silicate envelope behind the metal swarm, through the silicate layer containing the metal swarm or less abundantly through their middle planes. Sections passing through the swarm of metals below or above the decorated core would never display any hint of decoration but show only spherule swarms with no apparent orientation (e.g., Fig. 1 in Zipfel et al., 1995) and will lead to wrong conclusions e.g., (Mittlefehldt et al., 1996). We have scrutinized by reflected light microscope tomography in three dimensions many orthopyroxene grains rich in metal spherules in all our four Acapulco PTS. Our study indicates that only grains sectioned through or close to their middle planes (prismatic, oblique or basal sections) show the expected metal-sulfide decorated cores. Such sections are by no means rare in Acapulco. Figure 17a is a reflected light photograph of an orthopyroxene with small metal spherules decorating its core exposed at the section surface. Figure 17b is a photograph of the same grain with the microscope focused below the section surface inside the interior of the orthopyroxene core, thus uncovering the hemispherical envelope of spherules in depth perfectly oriented around the core. Figure 18 displays a reflected light photograph of another orthopyroxene where the polished surface is fortuitously a section through its middle plane. This figure unambiguously reveals the expected decoration of the metal spherule swarm around the orthopyroxene core. Figures 17 and 18 show that metals perfectly decorate the cores of orhopyroxene grains, thus confirming the reports of Palme et al. (1981) and Zipfel et al. (1995). The textural caveats raised by Mittlefehldt et al. can thus be easily dismissed (Mittlefehldt et al., 1996). We emphasize here that a partial melting process as proposed by Palme et al. (1981) and Zipfel et al. (1995) should also liberate and fragment graphites from the matrix metals. These graphite fragments would be enclosed in the metal spherules floating in the melt and deposited on the residual orthopyroxene and olivine cores. If this is the case, their average C- and N-isotopic compositions are expected to agree with those of the graphite morphologies in the matrix metals, the matrix graphite and the silicate melt (see 4.7 below).

Feldstein et al. (2001) recently conducted disequilibrium-melting experiments on the Leedey L6 chondrite to investigate the textural and compositional changes that take place during disequilibrium partial melting of chondritic meteorites. Metal melt globules were present in their one-hour experiment, for the most part associated with silicate melt and in general adherent to the residual solid silicate. These authors also found Fe-Ni-S globules enclosed by recrystallized orthopyroxene in experiments lasting longer than three days (their Fig. 4g). We stress the fact that the metal-sulfide textures produced in these experiments are completely different from those present in Acapulco

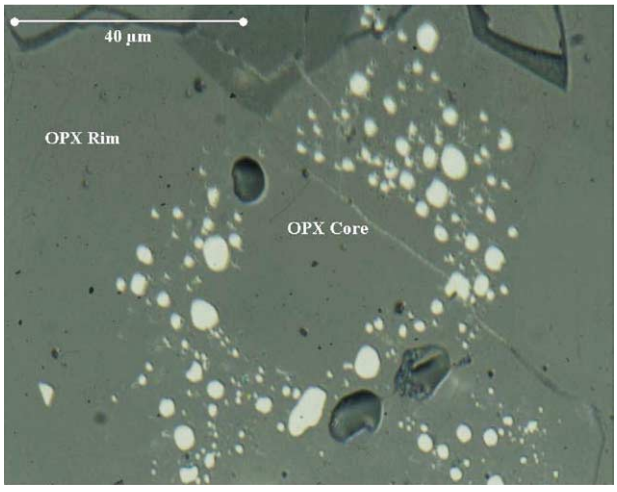

Fig. 18. Reflected light photograph of an orthopyroxene grain with perfect swarm decoration of metal spherules around its core (OPX core).

shown in our Figures 17 and 18 and previously reported from other acapulcoites before (Palme et al., 1981; Zipfel et al., 1995). In fact, none of the experiments conducted by (Feldstein et al., 2001) ever reproduced the decoration of metals around residual orthopyroxene cores like those as shown in our Figures 17, and 18. Their cited Figure 4g in the 7-d experiment displays randomly distributed metal spherules in neighboring olivine and orthopyroxene and at the border between them. Furthermore, their proposed diffusive equilibration model can never, via recrystallization, induce metal-sulfide spherule diffusion that would let the entire collection of the solid spherules migrate inside individual Mg-silicate crystals. A proposed "diffusion" scenario that would first, completely clean the outer rims of the orthopyroxene and olivine grains from metal and sulfide globules and, second, lead to migration of these solid objects to decorate similar imaginary sharp boundaries within single crystals of both orthopyroxenes and olivines. We remind here that these are minerals with different chemical compositions and crystal structures and yet according to the interpretation of (Feldstein et al., 2001) diffusion of solid metal spherules in orthopyroxene and olivine in Acapulco and in other acapulcoits, would produce exactly the same decoration pattern. If diffusion was the active mechanism, then why this diffusion of spherules didn't continue to reveal random distribution across orthopyroxenes and olivines and why in the first place the diffusion terminated around identical imaginary surfaces in both silicates?

4.4. Troilite-Orthopyroxene Symplectites

Melting of chondritic material produces two immiscible liquids, a silicate-dominated melt and a sulfide-metal liquid, and leaves behind solid restite minerals consisting mainly of pyroxenes and chromite (Jurewicz et al., 1995). Metal-sulfide droplets will be partially entrapped in crystallizing silicates and quenched silicate melt (Feldstein et al., 2001). The majority of troilite and the melted metal should, however, coalesce into

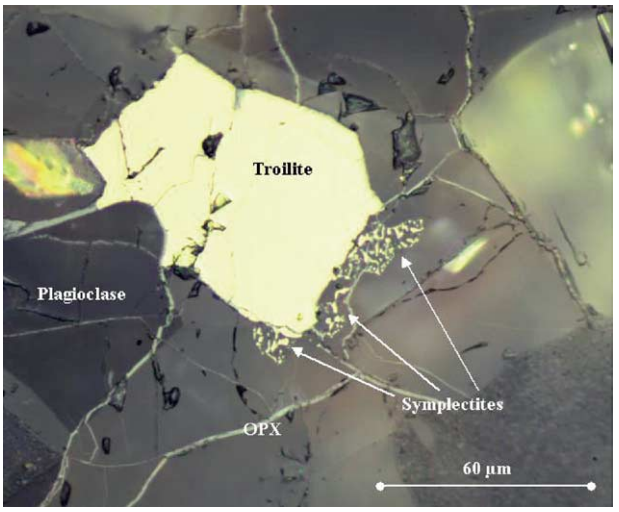

Fig. 20. Reflected light micrograph depicting orthopyroxene-troilite symplectite in orthopyroxene from the new Antarctic acapulcoite MET 01 195,11.

individual troilite or FeS-metal grains. Quenching and entrapment of some troilite and metal-silicate textures like symplectites are expected during orthopyroxene growth from the silicate-sulfide liquid around restite nuclei should silicate melting in Acapulco have taken place as proposed by Palme et al. (1981) and Zipfel et al. (1995). Indeed, we encountered such troilite symplectites entirely enclosed in orthopyroxene crystals in several Acapulco sections (Fig. 19). This texture unambiguously indicates that troilite and orthopyroxene simultaneously crystallized from a silicate-sulfide melt. Another symplectite in a new Antarctic acapulcoite (MET 01 195,11) contains not only troilite (Fig. 20) but also syplectite intergrowths of both troilite and chromite with orthopyroxene (Fig. 21). Similar textures of an unknown silicate and troilite were also reported from Lodran by (McCoy et al., 1997a) (their Fig. 4). Sulfide-silicate sym-

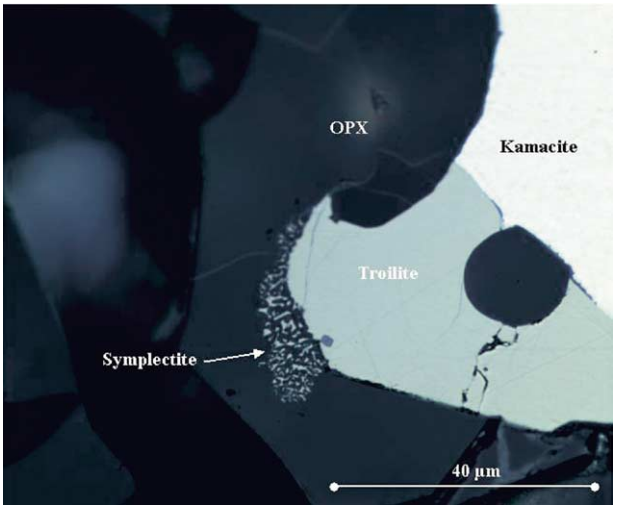

Fig. 19. Reflected light micrograph of a metal-troilite-orthopyroxene intergrowth. The troilite grain is decorated on its left side with a fine-grained troilite-orthopyroxene symplectite intergrowth that was quenched from a silicate-troilite melt.

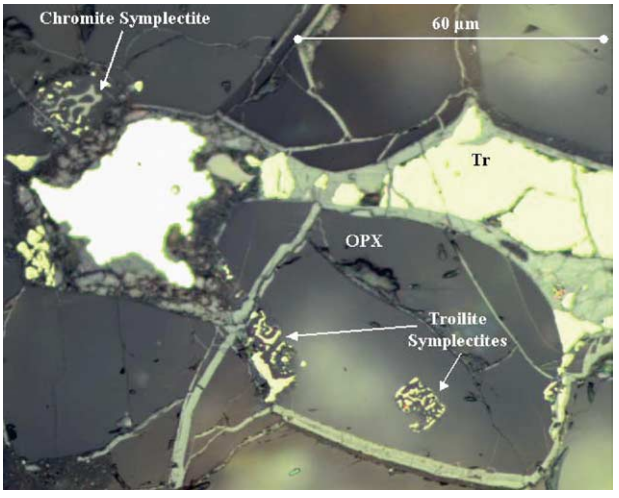

Fig. 21. Reflected light micrograph of an intergrowth of metal, troilite and chromite from the new Antarctic acapulcoite MET 01 195,11. Orthopyroxene contains troilite-orthopyroxene and troilite-chromite-orthopyroxene symplectites.

plectitic intergrowths are well known from numerous terrestrial occurrences to have formed by quenching during cooling of immiscible liquids (Ramdohr, 1980). Chromite-silicate symplectites were reported from ordinary chondrites in many chondrules that undoubtedly crystallized from a silicate-chromite melt (see e.g., Figures C18 and C19 in Ramdohr, 1973). Our findings demonstrate unambiguously that partial melting of not only silicates and troilite but also some chromite had taken place during the evolution of the acapulcoites, a fact that has been questioned by several authors (Mittlefehldt et al., 1996; McCoy et al., 1996; McCoy et al., 1997a; 1997b). Symplectites are quite rare in acapulcoites but can be located by systematic high-magnification microscopic search in reflected light. It is well known that metal-sulfide melts are quite mobile and coalesce into individual composite grains in a laboratory time scale (Kullerud, 1963). While the overwhelming majority of the sulfide liquid crystallized into coalesced individual grains, only a small fraction was entrapped as sulfide-orthopyroxene symplectite in the growing orthopyroxene rims, thus paying witness to the fact that sulfide-silicate melting in Acapulco and in MET 01 195,11 indeed took place. The presence of chromite-orthopyroxene symplectite is additional evidence that, due to heterogeneous temperature distribution on a millimeter scale, in certain parts of these meteorites some chromite was melted and entrapped in the growing rims of the orthopyroxenes as symplectite but not in orthopyroxene grains several hundreds of microns away. The high abundance of troilite and the lack of troilite veins between silicates in Acapulco (except next to the fusion crust) and in MET 01 195,11 indicate that no or very little sulfide entrainment and migration took place. More will be said about this topic in section 4.6.

The trigger for heat that led to partial melting in the acapulcoite-lodranite parent asteroid was discussed in several articles in the past (Palme et al., 1981; Zipfel et al., 1995; McCoy et al., 1996; McCoy et al., 1997b). Petrologic and geochemical studies (Palme et al., 1981; Zipfel et al., 1995; McCoy et al., 1996) convincingly negate an impact-induced partial melting. Acapulco mineral constituents display no shock features or high-pressure phase transitions, well known from many shocked and shock-melted L6 chondrites. These diagnostic features for shock-induced deformation and melting were never encountered in any acapulcoite or lodranite so far. We hence consider shock as the trigger for melting in the parent asteroid to be very unlikely. Localized heating through decay of short-lived isotopes (e.g., ^{60}Fe) seams to be a possible mechanism. There is enough growing evidence for live ^{60}Fe in the early evolution history of chondritic meteorites (Mostefaoui et al., 2003; Huss and Tashibana, 2004; Mostefaoui et al., 2004). This intense heat source should be capable of inducing massive melting in asteroids of several tens of kilometers in diameter.

4.5. Ir/Ni Ratios of The Decorated Metal Spherules In Comparison to the Ratios in Metals from Chondrules

The Ni/Ir ratio of the metal spherules in Acapulco (8.46×10^4) is more than a factor of 5 higher than the Ni/Ir ratio (1.5×10^4) of the large interstitial FeNi matrix metal (Zipfel et al., 1995). Zipfel et al. (1995) reported for the inclusions in orthopyroxenes and olivines a nearly H-chondritic Ni/Co ratio (18.8) that is similar to that in bulk samples. The Ni/Au ratio reported by the same authors is on average similar to the H-chondrite ratio of 7.44×10^4. In contrast, the Ni/Ir ratio is a factor 3 to 9 higher in the metal spherule inclusions in ortopyroxenes and olivines than in bulk Acapulco. They concluded that partial melting of Acapulco matrix metal could explain the Ni/Ir fractionation of the metal spherules, since Ir has the tendency to remain in the residual solid metal during partial melting. Mittlefehldt et al. (1996) questioned the Zipfel et al. (1995) model and argued that the Ni/Ir ratio of metals in LL chondrite chondrules is, on average, higher than the mean value of LL chondrites (Grossman and Wasson, 1985; Wasson and Kallemeyn, 1988). We emphasize that such a comparison between compositions of metals in LL-chondrites and in Acapulco can never clarify this dispute. Notwithstanding, we plot Ni and Ir abundances measured by Grossman and Wasson (1985) in Semarkona chondrules and compare them with the Ni/Ir ratios in Acapulco matrix metal and metal spherules in orthopyroxes (Fig. 22). The Ni/Ir ratios in Semarkona chondrules show considerable scatter but they plot, with few exception, closer to the ratio in Acapulco matrix metals (Fig. 22) Consequently, a comparison between Ni/Ir ratios in LL-chondrules and the Ni/Ir ratios of metal inclusions in Acapulco orthopyroxenes does not support a chondrule origin of the

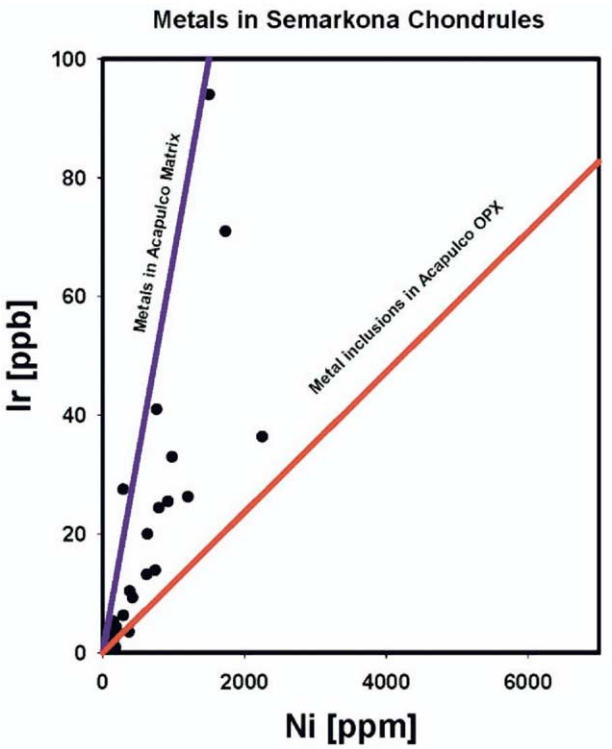

Fig. 22. A plot of the Ni and Ir abundances measured by (Grossman and Wasson, 1985) in Semarkona chondrules (filled black circles) in comparison with the Ni/Ir ratios in matrix metal (line on the left) and metal inclusions in orthopyroxes (line on the right) in Acapulco measured by (Zipfel et al., 1995). Note that the ratios in Samarkona metal deviate from the ratios of the metal inclusions in the Acapulco meteorite.

metal-sulfide inclusions in orthopyroxene or olivine in Acapulco.

4.6. Metal Patches and Troilite Veinlets and their Relevance to the Proposed Melt Migration Model

Our detailed search for metal and troilite veinlets in Acapulco revealed that troilite veinlets are present only in one section and they are spatially restricted to a 200 μm wide area below the fusion crust. Hence, they were produced near the fusion crust during the passage of the meteorite through the Earth's atmosphere and not during the partial melting of Acapulco in its parent body. The other sections, from an interior portion, are entirely barren of troilite or metal veins. We hence caution that samples cut from parts close to the fusion crust in which the fusion crust is invisible at the section surface because it is lying below, above or in close vicinity to the section surface, would feign pristine troilite veins. Fusion-crust-related troilite veins would be relatively more abundant in small meteorites, feigning pristine veins. The presence of veins filled with hydrated iron oxides in Antarctic meteorites or Saharan finds can never be used as evidence that they resulted from in situ weathering of preexisting troilite-metal veins. Weathering of FeNi metals in meteorite finds, regardless if in Antarctica or arid regions, leads to migration of hydroxide-bearing liquids and to precipitation of iron hydroxides in open cracks also elsewhere. Only the presence of pristine troilite and/or metal intergrown with hydrated iron oxides in veins in regions not related to the fusion crust is a reliable evidence for melt migration. We emphasize that the presence of troilite veins is convincing evidence since stoichiometric troilite is extremely resistant to weathering (Ramdohr, 1973; 1980). A recent study of several sections of Monument Draw indicated the presence of large metal patches but not veins. Every patch consists mostly of a single crystal of FeNi with prominent coarse plessite texture (Chen and El Goresy, 2005). Individual polygonal single troilite crystals are attached to the surface of the metal patches and decorate them. This texture is not reminiscent of melt veins. Details on their texture, composition and possible origin will be published elsewhere.

4.7. C- and N-Isotopic Compositions of Graphite Morphologies in Acapulco and Other Lodranites and their Relevance for the Evolution of the Meteorites' Parent Body

A crucial question is whether the measured *N*-isotopic compositions of the analyzed graphites are indigenous to Acapulco or the result of terrestrial contamination. We discussed this problem in detail in Section 2 on Analytical Methods and presented arguments against the possibility that the N isotopic variations measured in the graphites of this study are caused by contamination.

We envisage that the four graphite populations resolved in Figure 16 as important evidence for four different preaccretionary sources. The slope of 3.25 of the spherulitic graphite may have resulted either through (1) mixing of two isotopically different reservoirs, one with isotopically light carbon and nitrogen, and the other with $\delta^{13}C$ and $\delta^{15}N$ values close to zero (El Goresy et al., 1995a); or (2) is the result of isotopic mass fractionation before accretion. The exsolution veneers are the only graphites formed in the Acapulco parent body during cooling and very probably preserve the pristine carbon and nitrogen isotopic compositions of the metals before accretion. Alternatively, and perhaps more likely, their isotopic signature could have resulted from C- and N-isotopic mass fractionation induced by the graphite exsolution. They are isotopically the lightest in nitrogen. Their narrow isotopic range is good evidence that the metals, but not the different graphites enclosed in them originated in one source region. Their very light N-isotopic composition also argues against equilibration after accretion between metals and other silicate constituents in Acapulco that have isotopically heavy nitrogen (Sturgeon and Marti, 1991; Kim and Marti, 1994). Only in two cases do we see evidence for isotopic exchange between spherulitic graphite (type 1) and the attached graphite exsolution veneers (sperulitic graphite 3 and 21, Figs. 5, 11 and 15). Evidently, isotopic equilibration between the different graphite types occurred only rarely on a microscopic scale. Isotopic equilibration of metals with silicates and chromite would have erased the very light N-isotopic signatures of the veneers. Equilibration of the metals with matrix graphite would have overprinted the light carbon isotopic signatures as well. One matrix graphite has a unique carbon isotopic composition in comparison to the other morphologies. This points to an entirely different source. We don't know if this isotopic signature is similar to those of silicates and chromite, because they are unknown. The difference between the nitrogen isotopic composition of matrix graphite ($\delta^{13}C = +14.3 \pm 2.4‰$, $\delta^{15}N = -103.4 \pm 10.9‰$) and that of silicates is an additional argument against equilibration of this graphite with the isotopically heavy nitrogen of the latter. All other graphite morphologies enclosed in the matrix metal show a narrow C-isotopic compositional range ($\delta^{13}C = -4.6 \pm 2.4‰$–$13.55 \pm 2.4‰$). However their N-isotopic compositions vary widely ($\delta^{15}N = -80.3 \pm 21.4‰$ and $-160.2 \pm 8‰$). All these results indicate that, with two exceptions, the various graphite morphologies carry pristine preaccretionary C- and N-isotopic signatures. Min et al. (2003) report single grain (U-Th)/He ages for phosphates in Acapulco that suggest rapid cooling of the meteorite to $\sim$ 120°C. Such a rapid cooling is probably responsible for the lack of isotopic exchange between graphite morphologies enclosed in the same metal grain.

In a previous study El Goresy et al. (1995a) report a $\delta^{13}C = -28 \pm 3‰$ for an isolated cohenite inclusion in a matrix metal in Acapulco. The difference in $\delta^{13}C$ between coexisting cohenite and graphite is well documented in several iron meteorites by Deines and Wickman (1975). Cohenite systematically shows isotopically lighter C than the coexisting graphite ($\delta^{13}C$ -18 to -21 ‰ vs. ≈ -6 ‰). This is because the compound with lower vibrational frequencies (or higher heat capacity) will concentrate the lighter isotope. Deines and Wickman (1975) convincingly interpreted this difference as reflecting the approach to isotopic equilibrium and to be due to isotopic fractionating properties of the phases involved. In Acapulco $\delta^{13}C$ values in both cohenite and graphite veneers are lower ($\delta^{13}C$ -28 ‰ in cohenite and -17 to -21 ‰ in graphite, respectively) than in iron meteorites, though the isotopic difference between the two phases is comparable to values obtained by Deines and Wickman in iron meteorites. Following Deines and Wickman's interpretation, one may conclude here

that the $\delta^{13}C$ value of Acapulco cohenite is possibly close to that of Acapulco taenite and hence taenite in Acapulco has isotopically lighter carbon than in iron meteorites. However, we add some caution, because the analyzed cohenite and graphite in Acapulco didn't coexist in the same metal grain and hence did not necessarily equilibrate with each other. Nonetheless, the data signal an overall lack of equilibrium, the result of rapid cooling (Min et al., 2003).

The C-and N-isotopic compositions of graphite inclusions in the metal spherules in orthopyroxene offer a critical test of their origin. The presence of the spherules was reported from all acapulcoites studied, thus indicating that their formation process was global in the region of the asteroid in which these meteorites formed. It is evident that the mineralogy of the metal-sulfide spherules enclosed in orthopyroxenes and olivines is not identical in different acapulcoites. While we find abundant phosphates and graphite in the metal spherules in Acapulco, they are entirely absent in the Monument Draw metal spherules (Chen and El Goresy 2005). This strongly suggests the existence of several unconnected partial melt pockets in the mineralogically heterogeneous acapulcoite source region in the parent body. This raises the question why melt drainage and exchange didn't then take place, as suggested for lodranites. The phase mineralogy of the metal spherules would have been similar in the studied acapulcoites if these pockets were interconnected and communicated through melt drainage and intermigration. A critical test of whether the metal spherules in pyroxenes were locally produced from the same Acapulco lithology and not introduced from another close or distant source by melt migration, is provided by the carbon and nitrogen isotopic signatures of graphite inclusions in the metal spherules in comparison with the isotopic compositions of graphite inclusions in matrix metals in the same meteorite. Carbon and nitrogen isotopic compositions of a graphite inclusion in a metal spherule should resemble the average isotopic compositions of graphite inclusions in matrix metals on the one hand, and graphite books in silicate matrix on the other, if they were locally produced during a partial melt process in the very source region of the given meteorite. A graphite in a metal spherule inside orthopyroxene has $\delta^{13}C = -2.9 \pm 2.5‰$ and $\delta^{15}N = -101.2 \pm 32‰$ (Fig. 16). Its nitrogen isotopic composition is close to the mean of all graphite morphologies studied, whereas its carbon isotopic composition lies at the heavy end of all graphite morphologies in matrix metals and closest to the graphite crystals in silicate matrix that is rich in heavy carbon (El Goresy et al., 1995a). This argues that the graphite inclusions in metal spherules are indeed pristine to Acapulco and that their C- and N-isotopic compositions fingerprint isotopic partial equilibration in the partial melt, i.e., the graphite inclusions picked up a heavy carbon isotopic signature from the silicate matrix graphites and accommodated their N-isotopic composition to the mean of all graphite morphologies in Acapulco. However, its N-isotopic composition does not indicate that it is equilibrated with the positive N-isotopic composition of the silicates during the partial melting event. However, we caution that the present study is the only one so far that scrutinized the phase mineralogy of the metal spherules in orthopyroxene and olivine in acapulcoites and determined the isotopic compositions of only one graphite inclusion in them. A careful petrographic and isotopic survey of graphite inclusions in such spherules in other members of this group is needed to further substantiate this result.

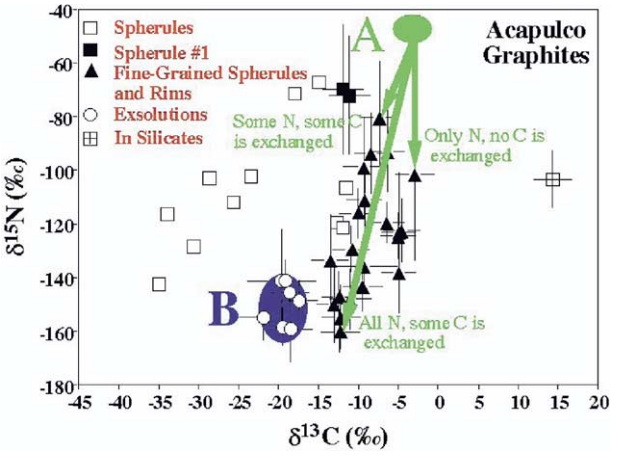

Fig. 23. A $\delta^{15}N$ vs. $\delta^{13}C$ isotope plot displaying the N and C-isotopic compositions of all graphite morphologies analyzed in the Acapulco samples shown in Figure 21 and the isotopic exchange scenario discussed in the text.

The present investigations suggest that at least three reservoirs are required to explain the diverse C- and N-isotopic compositions of the graphite types in Acapulco: (1) A reservoir with heavy carbon represented by graphite in silicates. (2) A reservoir with isotopically light C ($\delta^{13}C = -17$ to $-23‰$) and N ($\delta^{15}N = -141$ to $-159‰$), characteristic of the metals before the inclusion of other graphite morphologies. Its C- and N-isotopic compositions are evidently preserved in the graphite exsolutions. (3) A reservoir with an assumed isotopic composition at the upper end of the spherulitic graphite array ($\delta^{13}C \sim -5‰$; $\delta^{15}N \sim -50‰$; Fig. 23). The true composition of the latter reservoir could possibly lie on the extension of the correlation line but our choice is based on the assumption that the isotopic composition of the isotopically heaviest spherulitic graphite (type 1) is close to the composition of this hypothetical reservoir. Isotopic partial or wholesale isotopic exchange between this postulated reservoir and the metal component could in principle explain the isotopic variations observed in the feathery, fibrous and fine-grained morphologies. It is yet unclear why individual graphite grains of each of these four morphologies would have experienced different degrees of isotopic exchange since the diffusion rates of C and N in all graphite morphologies should be similar for a given fO_2 and temperature. Differences in the isotopic exchange rates could have resulted from variations in fO_2 and/or temperature but the postulated exchange must then have taken place before incorporation of the various graphite morphologies into Acapulco and definitely before partial melting and recrystallization of the Acapulco local source region. At any case, the decoration of the metal and sulfide spherules around the cores of orthopyroxenes and olivines indicate that decoration took place during an early and very local partial melting process with no melt drainage or migration to or from other sources. The C- and N-isotopic signature of graphite inclusions in these spherules therefore reflects an average of the graphites in the Acapulco source region.

Isotopic studies of graphites in acapulcoites and lodranites

are quite scarce. Recent isotopic studies of graphites in the lodranite Graves Nunatakes revealed large variations in their δ^{13}C-isotopic compositions by 86‰ ($\delta^{13}C = -36 \pm 6$‰ to $+ 50 \pm 6$‰) in graphites separated by only 60 μm (Nittler and McCoy, 2000). Yet it is unclear why the normal nitrogen isotopic composition of graphites in this lodranite should be the result of adsorption of terrestrial nitrogen as (Nittler and McCoy, 2000) conclude. We raise here the question why such equilibration didn't take place in Acapulco graphites, which were subjected to temperatures close to or in excess of ~1000°C. We maintain that our results indicate a high degree of isotopic retentivity of graphite at high temperatures, a property that should persist at much lower temperatures. We argue that the graphites in acapulcoites and lodranites contain a fingerprint of the pristine local lithology of these individual meteorites. A detailed isotopic study of graphites in other acapulcoites and lodranites is needed to elucidate the genetic links between these meteorites that may lead to common source regions for many of them.

5. DEGREE OF PARTIAL MELTING AND MELT-ENTRAINMENTS

Depletion of some lodranites in plagioclase, phosphates and Fe-FeS, in REE and some incompatible elements such as Ti, Zr and Y have been attributed to partial melting and melt migration (Nagahara, 1992; Torigoye et al., 1993; Mittlefehldt et al., 1996; McCoy et al., 1997a; Floss, 2000). Many acapulcoites do not show similar depletions (Palme et al., 1981; Zipfel et al., 1995; Mittlefehldt et al., 1996; McCoy et al., 1997a; McCoy et al., 1997b). This apparent dichotomy was considered by some authors as evidence for the lack of or the presence of only minor partial melts in acapulcoites (Mittlefehldt et al., 1996; McCoy et al., 1996; McCoy et al., 1997a; McCoy et al., 1997b), with the argument that partial melting should plausibly imply subsequent melt migration (Mittlefehldt et al., 1996). Phosphate veins in Monument Draw were attributed to melting and migration of phosphates and in situ crystallization of melts in open cracks (McCoy et al., 1996). The REE abundances in these phosphates indicate lack of equilibrium (McCoy et al., 1996). Detailed investigations also demonstrated abundant heterogeneity in acapulcoites and lodranites, thus indicating high complexity of petrologic processes on a small spatial scale, as can, e.g., be seen in LEW 86220 (McCoy et al., 1997a). Another important case demonstrating the complexity of partial melting and entrainment processes is EET 84302, a meteorite classified by (McCoy et al., 1997a) as a lodranite but classified by (Floss, 2000) as being transitional between acapulcoites and lodranites. The REE patterns of merrilite in this meteorite do not show the LREE depletions typical of calcium phosphates from lodranites (Floss, 2000). In addition, while e.g., troilite is depleted in EET 84302, plagioclase is present in approximately chondritic abundance (McCoy et al., 1997a). This meteorite, as well as ALHA 81187 and GRA 95209 present classical cases that show the complexity of silicate-sulfide melt evolution that perhaps consisted of sulfide melt drainage followed by limited silicate melt loss (Floss, 2000). However, migration of plagioclase melts within its own region cannot be excluded to account for the observed trace element patterns. These meteorites have recently been classified as transitional that were subjected to silicate partial melting with most of the melts probably having crystallized in situ (Floss, 2000). In short, melting processes, melt drainage and intermigration on a small spatial scale are processes that are too complex to allow a straightforward delineation of the evolution history of all members of the group from the REE abundances alone. The recent article by (Floss, 2000) has outlined many of the problems that plagued a simple bimodal classification model in acapulcoites and lodranites. She introduced a modified model to account for the observed differences, yet there are many unresolved issues. Notwithstanding, a partial silicate melt in Acapulco was considered highly unlikely under the assumption that metal-troilite spherules in orthopyroxenes and olivines were not produced by partial melting of silicate components (Mittlefehldt et al., 1996; McCoy et al., 1996; McCoy et al., 1997a; McCoy et al., 1997b; Feldstein et al., 2001). These authors also argued that partial melting should be plausibly followed by melt drainage, as apparently is the case in many lodranites. The evidence presented above in 4.1 to 4.7 unambiguously demonstrates that, contrary to the interpretations by (Mittlefehldt et al., 1996; McCoy et al., 1996; McCoy et al., 1997a; McCoy et al., 1997b; Feldstein et al., 2001), Acapulco was indeed subjected to a partial metal-sulfide-silicate melting event with closed-system crystallization but with no melt drainage or migration. This melting event was followed by solid-state recrystallization, which erased the majority of preexisting igneous textures, whereby entrapped symplectite and metal spherules-decoration textures that had resulted from the in situ partial melting process were preserved (see 4.3 and 4.4). Measurements of REE and other incompatible elements in the rims and cores of orthopyroxenes in Acapulco containing metal spherules by NanoSIMS as proposed by (Floss, 2000) should reveal differences in the REE and incompatible element concentrations, if the rims crystallized from a silicate mesh around the residual nuclei (Zipfel et al., 1995). However, such an experiment is beyond the scope of the present article. It appears that the building stones of the acapulcoite-lodranite parent body were individually subjected to a variety of processes including solid-state recrystallization, partial melting of metal-troilite, phosphates and plagioclase, whereby in some cases closed-system crystallization took place while in others only metal-sulfide melts were entrained. Almost complete migration of the metal-sulfide-phosphate-plagioclase melts was also achieved in some members, e.g., in many lodranites. A simple strict bimodal classification model cannot explain the variety of petrological and geochemical features observed (Floss, 2000).

6. CONCLUSIONS

Our investigations on the Acapulco meteorite revealed new information that is crucial for unraveling the evolutionary history of this meteorite from preaccretionary stages to thermal events in the acapulcoite-lodranite parent body. Various morphologies of accessory graphite are present, as inclusions in FeNi metal grains, as exsolution between kamacite and taenite in individual metal grains, and as individual graphite crystals in the silicate matrix. The graphites display a diversity of C- and N-isotopic compositions and can be divided into four isotopically distinct groups. The carbon and nitrogen isotopic variations of the graphite morphologies indicate three different

preaccretionary sources with distinct C- and N-isotopic signatures. Graphite exsolution veneers separating kamacite from taenite are isotopically lightest in N and their C- and N-isotopic compositions may preserve the primordial isotopic composition of the FeNi metal. Specifically, their presence between the two metals indicates that Ni and Fe diffusion between kamacite and taenite was impeded or even inhibited at some stage during cooling in the parent body. As a consequence, Ni-compositional profiles across metal grain boundaries in Acapulco cannot be used for estimating metallographic cooling rates. Metal-sulfide spherules in orthopyroxene and olivine concentrically decorate restite cores of these minerals. Some metal spherules contain graphite specks whose C- and N-isotopic compositions are similar to the average isotopic compositions of graphites in metal and silicate matrix, thus indicating that the spherules originated from parental matrix metals during a local melting process in Acapulco. Orthopyroxene-troilite symplectites in the outer rims of some orthopyroxenes were formed in a local closed system during silicate-sulfide partial melting. Contrary to previous reports, troilite veins in the Acapulco meteorite are confined to a narrow zone below the fusion crust. Hence, these veins were formed by troilite melting and mobilization during passage of Acapulco through the Earth's atmosphere and not on its parent body. Our investigations indicate that Acapulco was subjected to a partial silicate-troilite-metal melting process followed by closed-system crystallization. This conclusion is in contrast to many previous reports on the thermal history of the Acapulco meteorite. The thermal event evidently did not overprint or homogenize the C- and N-isotopic compositions of the various graphite morphologies. Study of the isotopic compositions of highly retentive graphites in the acapulcoilte-lodranite clan should reveal important genetic information on the evolution of the parent body.

Acknowledgments—We are grateful to J. Huth, I. Bambach and G. Feyerherd of the Max-Planck-Institut für Chemie in Mainz, Germany for careful scanning of the SEM figures thus reproducing them in excellent quality. The manuscript have benefited considerably through constructive reviews by H. Palme, K. Marti and an anonymous reviewer and advice from Associate Editor Alexander Krot.

Associate editor: A. N. Krot

REFERENCES

Brett R. and Higgins G. T. (1967) Cliftonite in meteorites: A proposed origin. *Science* **156,** 819–820.

Brett R. (1967) Cohenite: its occurrence and proposed origin. *Geochim. Cosmochim. Acta* **31,** 143–159.

Chen M. and El Goresy A. (2005) The Monument Draw acapulcoite, revisited. *Meteorit. Planet. Sci.*, in preparation.

Clayton R. N., Mayeda T. K. and Nagahara H. (1992) Oxygen isotope relationship among primitive achondrites. *Lunar Planet. Sci.* **XXIII**, 231–232.

Clayton R. N., Mayeda T. K. and Yanai K. (1984) Oxygen isotopic compositions of some Yamato Meteorites. *Proc. 9th Symp. Antarct. Meteorit.* 267–271.

Deines P. and Wickman F. E. (1975) A contribution to the stable carbon isotope geochemistry of iron meteorites. *Geochim. Cosmochim. Acta* **39,** 547–558.

El Goresy A. and Janicke J. (1995) Diverse chemical zoning trends in Acapulco chromites: How many sources for the parental materials? *Meteorit. Planet. Sci.* **30,** 503–504.

El Goresy A., Zinner E. and Marti K. (1995a) Survival of isotopically heterogeneous graphite in a differentiated meteorite. *Nature* **373,** 496–499.

El Goresy A., Zinner E., Pellas P. and Caillet C. (1995b) Acapulco's graphite menagerie: Diverse carbon and nitrogen isotopic signatures. *Lunar Planet. Sci.* **XXVI**, 367–368.

Feldstein S. N., Jones R. H. and Papike J. J. (2001) Disequilibrium partial melting experiments on the Leedey L6 chondrite: textural controls on melting processes. *Meteorit. Planet. Sci.* **36,** 1421–1441.

Floss C. (2000) Complexities on the acapulcoite-lodranite parent body: Evidence from trace element distributions in silicate minerals. *Meteorit. Planet. Sci.* **35,** 1073–1085.

Franchi I. A., Akagi T. and Pillinger C. T. (1992) Laser fluorination of meteorites—Small sample analysis of $\delta^{17}O$ and $\delta^{18}O$. *Meteorit. Planet. Sci.* **27,** 2219.

Grossman J. N. and Wasson J. T. (1985) The origin and history of the metal and sulfide components of chondrules. *Geochim. Cosmochim. Acta* **49,** 925–939.

Huss G. R. and Tashibana S (2004) Clear evidence for 60Fe in silicate from a Semarkona chondrule. *Lunar Planet. Sci.* **XXXV**, 1811.

Jurewicz A., Mittlefehldt D. W. and Jones J. (1995) Experimental partial melting of the St. Severin (LL) and Lost City (H) chondrites. *Geochim. Cosmochim. Acta* **59,** 391–408.

Kim Y. and Marti K. (1994) Genetic relationship of acapulcoites and lodranites? A study of nitrogen and xenon isotopic signatures *Lunar Planet. Sci.* **XXXV**, 703–704.

Kullerud G. (1963) The Fe-Ni-S system. In *Carnegie Institution of Washington, Yearbook*, pp. 175–189.

Maruoka T., Kurat G., Zinner E., Varela M. E. and Ametrano S. J. (2003) Carbon isotopic heterogeneity of graphite in the San Juan mass of the Campo del Cielo IAB iron meteorite. *Lunar Planet. Sci.* **XXXIV**, 1663.

McCoy T. J., Keil K., Clayton R. N., Mayeda T. K., Bogard D. D., Garrison D. H., Huss G. R., Hutcheon I. D. and Wieler R. (1996) A petrologic, chemical and isotopic study of Monument Draw and comparison with other acapulcoites: Evidence for formation by incepient partial melting. *Geochim. Cosmochim. Acta* **60,** 2681–2708.

McCoy T. J., Keil K., Clayton R. N., Mayeda T. K., Bogard D. D., Garrison D. H. and Wieler R. (1997a) A petrologic and isotopic study of lodranites: Evidence for early formation as partial melt residues from heterogeneous precursors. *Geochim. Cosmochim. Acta* **61,** 623–637.

McCoy T. J., Keil K., Muenow D. W. and Wilson L. (1997b) Partial melting and melt migration in the acapulcoite-lodranite parent body. *Geochim. Cosmochim. Acta* **61,** 639–650.

Min K., Farley K. A., Renne P. R. and Marti K. (2003) Single grain (U-Th)/He ages from phosphates in Acapulco meteorite and implications for thermal history. *Earth Planet. Sci. Lett.* **209,** 323–336.

Mittlefehldt D. W., Lindstrom M. M., Bogard D. D., Garrison D. H. and Field S. (1996) Acapulco- and Lodran-like achondrites: petrology, geochimstry, chronology and origin. *Geochim. Cosmochim. Acta* **60,** 867–882.

Mostefaoui S., Zinner E., Hoppe P., Stadermann F. and El Goresy A. (2005) In situ survey of graphite in unequilibrated chondrites: morphologies, C, N, O and H isotopes. *Meteorit. Planet. Sci.* **40**, 721–744.

Mostefaoui S., Lugmair G. W., Hoppe P. and El Goresy A. (2003) Evidence for live iron-60 in Semarkona and Chervony Kut: A Nanosims study. *Lunar Planet. Sci.* **XXXIV**, 1585.

Mostefaoui S., Lugmair G. W. and Hoppe P. (2004) In-situ evidence for live iron-60 in the Early Solar system: Potential heat source for planetary differentiation from a nearby supernova explosion. *Lunar Planet. Sci.* **XXXV**, 1271.

Nagahara H. (1992) Yamato-8002: Partial melting residue on the "unique" chondrite parent body. *Proc. of NIPR Symp. Antarct. Meteorit.*191–223.

Nakamura T., Hoppe P. and El Goresy A. (2005) Diverse Carbon and Nitrogen isotopic compositions of graphites in three new Acapulcoites. *Geochim. Cosmochim. Acta* In preparation.

Nittler L. R. and McCoy T. J. (2000) Carbon isotopes in graphite from Lodranite Graves Nunatakes 95209. *Meteorit. Planet. Sci.* **35,** A120.

Pack A., Hetzel D. and El Goresy A. (2005) SIMS study of Si and P-contents of metals in acapulcoites: Implications to evaluation of metallographic cooling rates. *Geochim. Cosmochim. Acta* In preparation.

Palme H., Schulz L., Spettel B., Weber H. W., Wänke H., Christophe Michel-Levy M. and Lorin J. C. (1981) The Acapulco Meteorite: Chemistry, mineralogy and irradiation effects. *Geochim. Cosmochim. Acta* **45,** 727–752.

Pellas P., Feini C., Trieloff M. and Jessberger E. (1997) The cooling history of the Acapulco meteorite as recorded by the ^{244}Pu and ^{40}Ar-^{39}Ar chronometers. *Geochim. Cosmochim. Acta* **61,** 3477–3501.

Ramdohr P. (1973) The Opaque Minerals in Stony Meteorites. Elsevier.

Ramdohr P. (1980) Die Erzmineralien und Ihre Verwachsungen. Akademie Verlag.

Reisner R. J. and Goldstein J. I. (2003a) Ordinary chondrite metallography: Part 1, Fe-Ni taenite cooling experiments. *Meteorit. Planet. Sci.* **38,** 1669–1678.

Reisner R. J. and Goldstein J. I. (2003b) Ordinary chondrite metallography: Part 2, Formation of zoned and unzoned metal particles in relatively unshocked H, L and LL chondrites. *Meteorit. Planet. Sci.* **38,** 1679–1696.

Schulz L., Palme H., Weber H. W., Wänke H., Christophe Michel-Levy M. and Lorin J. C. (1982) Alan Hills 77081—an unusual stony meteorite. *Earth Planet. Sci. Lett.* **61,** 23–31.

Stroud R. M., Nittler L. R. and McCoy T. J. (2001) Microstructure of graphite with unusual carbon isotopes in lodranite Graves Nunataks 95209. *Meteorit. Planet. Sci.* **36,** A200.

Sturgeon G. and Marti K. (1991) Nitrogen isotopic signatures in the Acapulco meteorite. *Proc. Lunar. Planet. Sci.* **21,** 523–525.

Torigoye N., Yamamoto K., Misawa K. and Nakamura N (1993) Compositions of REE, K, Rb, Sr, Ba, Mg, Ca, Fe and Sr isotopes in Antarctic "unique" meteorites. *NIPR Symp. Antarct. Meteorit.* 100–119.

Wasson J. T. and Kallemeyn G. W. (1988) Compositions of chondrites. *Phil. Trans. Roy. Soc. Lond.* **A 325**, 535–544.

Zinner E., Tang M. and Anders E. (1989) Interstellar SiC in the Murchison and Murray meteorites: Isotopic composition of Ne, Xe, Si, C and N. *Geochim. Cosmochim. Acta* **53,** 3273–3290.

Zipfel J., Palme H., Kennedy A. K. and Hutcheon I. D. (1995) Chem. composition and origin of the Acapulco meteorite. *Geochim. Cosmochim. Acta* **59,** 3607–3627.

APPENDIX 1

CN−/C− and isotopic compositions of spherulitic, feathery and other graphite morphologies in the Acapulco meteorite (data from El Goresy et al., 1995a).

delta-13C	error	delta-15N	error	CN−/C−
Spherulitic				
−33.9	2.1	−116.1	9.2	0.0109
−25.7	2.1	−112	10.3	0.0088
−23.4	2.2	−102.1	9.4	0.0103
−11.5	2.1	−106.4	11.2	0.0075
−11.9	2.1	−121.3	7.3	0.0182
−28.7	2.1	−102.9	12.1	0.0081
−18	2.2	−71.5	8	0.0068
−30.7	2.3	−128.2	10.4	0.0108
−12.7	2.2	−119.2	12.7	0.0086
−34.9	2.1	−142.2	16	0.0063
−15	2.1	−67.1	9.6	0.0163
Feathery				
−9.1	2.1	−154.6	8.7	0.0116
−14	2.1	−123.4	8.1	0.0136
−11.8	2.1	−149.5	7.8	0.0154
−9.1	2.2	−146.6	7.3	0.0171
−19.7	2.1	−123.3	6.7	0.0208
−10.3	2.2	−141.3	7.7	0.0166
−11.9	2.1	−121.3	7.3	0.0182
−12.8	2.2	−110.2	9.3	0.0165
−9.7	2.4	−106.4	7	0.0279
−13.2	2.2	−128.4	9.5	0.0142
−8.9	2.4	−128.1	15.8	0.0082
−8.1	2.2	−112.5	7.8	0.0207
Other				
−15	2.1	−121.8	6.8	0.0321
−11.2	2.2	−115.5	8.3	0.0139

APPENDIX 2

Morphologies, CN/C− ratios and isotopic compositions of graphites in the Acapulco meteorite.

Measurement spot	Morphology	delta-^{13}C	error	delta-^{15}N	error	CN−/C−
GRAPH-1-A.1	Spherulitic	−11.1	2.73	−71.99	22.28	0.0027
GRAPH-1-B.1	Fibrous	−10.99	2.69	−147.98	11.43	0.0152
GRAPH-1-B.2	Fibrous	−9.47	2.6	−143.05	9.82	0.0142
GRAPH-1-C.1	Exsolution Veneer	−18.51	2.88	−159.04	12.55	0.0306
GRAPH-1-D.1	Spherulitic	−11.91	2.6	−69.9	24.53	0.0019
GRAPH-10-A.1	Fine-grained	−12.45	2.25	−146.97	9.59	0.012
GRAPH-10-B.1	Exsolution Veneer	−10.95	2.39	−129.47	8.79	0.0338
GRAPH-10-C.1	Exsolution Veneer	−19.16	2.46	−141.29	8.26	0.0521
GRAPH-13-A.1	Fine-grained	−9.24	2.29	−110.87	10.03	0.0128
GRAPH-14-A.1	Matrix Books	14.34	2.44	−103.36	10.88	0.0147
GRAPH-16-A.1	Fine-grained	−4.56	2.37	−122.44	12.22	0.0081
GRAPH-16-B.1	Fibrous	−5.01	2.31	−124.26	8.86	0.0258
GRAPH-17-A.1	Spherulitic	−8.35	2.31	−93.74	15.25	0.0052
GRAPH-17-A.2	Spherulitic	−4.93	2.3	−122.76	22.18	0.0045
GRAPH-17-A.3	Spherulitic	−4.9	2.29	−138.27	15.13	0.0041
GRAPH-17-B.1	Exsolution Veneer	−9.27	4.32	−135.68	10.69	0.0463
GRAPH-18-A.1	Fine-grained	−6.35	2.29	−92.82	15.43	0.0049
GRAPH-18-B.1	Exsolution Veneer	−6.39	2.33	−119.3	7.69	0.0295
GRAPH-2-A.1	Spherulitic	−13.55	2.43	−133.47	17.25	0.0058
GRAPH-2-B.1	Exsolution Veneer	−12.33	2.55	−160.18	8	0.0237
GRAPH-21-A.1	Spherulitic	−23.39	2.24	−148.91	6.93	0.0254
GRAPH-21-B.1	Exsolution Veneer	−17.46	2.5	−148.65	7.73	0.0489
GRAPH-21-B.2	Exsolution Veneer	−19.53	2.48	−158.28	7.25	0.0578
GRAPH-21-C.1	Exsolution Veneer	−21.92	3.06	−154.9	8.46	0.0672
GRAPH-3-A.1	Spherulitic	−21.63	2.29	−147.85	13.35	0.0092
GRAPH-3-B.1	Exsolution Veneer	−19.61	4.36	−141.3	19.51	0.0879
GRAPH-5-A.1	Fine-grained	−12.96	2.34	−149.64	14.79	0.0061
GRAPH-5-B.1	Fibrous	−7.34	2.35	−80.31	21.38	0.0044
GRAPH-6-A.1	Fine-grained	−9.38	2.74	−98.78	18.84	0.0037
GRAPH-7-A.1	Fine-grained	−10.16	2.32	−116.11	9.45	0.0132
GRAPH-7-B.1	Exsolution Veneer	−18.6	2.45	−145.65	6.85	0.0531
GRAPH-9-A.1	Exsolution Veneer	−12.2	2.55	−154.71	12.3	0.0279
GRAPH-B.1	In metal Spherule in orthopyroxene	−2.93	2.45	−101.25	32.42	0.0016